Synthesis of Dibenzo[*hi,st*]ovalene and Its Amplified Spontaneous Emission in a Polystyrene Matrix

Giuseppe M. Paternò[‡,[a]] Qiang Chen[‡,[b]] Xiao-Ye Wang,[b] Junzhi Liu,[c] Silvia G. Motti,[a] Annamaria Petrozza,[a] Xinliang Feng,[c] Guglielmo Lanzani,[a,d] Klaus Müllen*,[b] Akimitsu Narita*[b] and Francesco Scotognella*[a,d]

Abstract

A large number of graphene molecules, or large polycyclic aromatic hydrocarbons (PAHs), have been synthesized displaying varying optoelectronic properties. Nevertheless, their potential for application in photonics has remained largely unexplored. Herein, we describe the synthesis of a highly luminescent and stable graphene molecule DBO 1 with zigzag edges and elucidate its promising optical gain properties by means of ultrafast transient absorption spectroscopy. The incorporation of DBO 1 into an inert polystyrene matrix permits to observe amplified stimulated emission with a relatively low power threshold (≈ 60 μJ cm-2), thus highlighting its high potential for lasing applications.

[a] Dr. G. M. Paternò, S. G. Motti, Dr. A. Petrozza, Prof. G.Lanzani
Center for Nano Science and Technology
Istituto Italiano di Tecnologia
20133 Milano (Italy)

[b] Q. Chen, Dr. X.-Y. Wang, Prof. K. Müllen, Dr. A. Narita
Max Planck Institute for Polymer Research
55128 Mainz (Germany)
email: muellen@mpip-mainz.mpg.de
email: narita@mpip-mainz.mpg.de

[c] Dr. J. Liu, Prof. X. Feng
Technische Universität Dresden, Center for Advancing Electronics Dresden & Department of Chemistry and Food Chemistry
01062 Dresden (Germany)

[d] Dr. F. Scotognella
Politecnico di Milano
Department of Physics
20133 Milano (Italy)
email: francesco.scotognella@polimi.it

[‡] These authors contributed equally to this work.

Supporting information for this article is given at the end of the document.

Along with the development and successful commercialization of organic light-emitting diodes, extensive research has been devoted to the search for stable organic semiconductors (OSCs) that can be employed as optical gain media in laser devices[1]. The reasons for targeting organic lasers are: 1) the excellent optical features exhibited by organic luminescent materials, 2) the tunability of their optoelectronic properties by means of structural modulation and 3) the high solution processability[2] that allows for the fabrication of low-cost devices. However, their considerable photodegradation upon intense laser irradiation and intrinsic instability against air and moisture are still major obstacles[1b].

Graphene materials have more recently emerged as promising alternative for stable luminescent systems. Although graphene itself has no bandgap, structural patterning into graphene nanostructures, i.e., nanographenes, such as quasi-one-dimensional graphene nanoribbons (GNRs)[3] and quasi-zero-dimensional graphene quantum dots (GQDs)[4] allows to open a finite bandgap owing to quantum confinement of the electronic wave function. While top-down fabrication methods cannot precisely control the size and edge structure of the resulting nanographenes, bottom-up chemical synthesis from small molecular building blocks has proven to provide GNRs and GQDs, or graphene molecules, with atomically defined structures[5]. Such nanographene materials, indeed, exhibit intriguing luminescence features[6] that depend strongly on the size and edge structures[7], making them of great interest for plasmonic[8] and photonic applications[9]. There have been a few reports demonstrating or implying stimulated emission (SE) signal from structurally defined GNRs[10] and graphene molecules[6a] by transient absorption (TA) measurements in dispersions, which suggests their possible application as optical gain materials. However, to the best of our knowledge, there is hitherto no unambiguous proof for the SE from graphene molecules, and moreover actual amplified spontaneous emission (ASE) of such nanographene materials has never been observed in films. ASE action would be, in fact, an extremely important effect with the perspective of their role as gain media in laser devices.

A variety of GNRs and graphene molecules featuring armchair-type edge structures have so far been synthesised[11], but examples with zigzag edges are still limited, despite their intriguing properties such as lowered energy gaps as well as biradical ground-state characters[12]. Furthermore, most of the reported zigzag-edged graphene molecules are highly unstable, hindering their in-depth characterisations and applications in devices[12b, 13]. In this work, we have synthesized dibenzo[*hi*,*st*]ovalene (DBO **1**) (Scheme 1) as a novel and stable graphene molecule with both armchair and zigzag edges. DBO **1** exhibits a small optical gap (1.93 eV) based on the UV-*vis* absorption spectrum and an absolute photoluminescence quantum yield (PLQY) of as high as 79%. The investigation of the excited state dynamics, carried out by means of resonant ultrafast TA spectroscopy, clearly reveals the occurrence of SE transitions in solution. Although the prominent optical properties of DBO **1** were largely quenched in the solid state, we were able to recover the SE signal by blending the molecule with polystyrene (PS), which, interestingly, led to the observation of ASE action from a 1 w% DBO **1** : PS composite film.

The synthesis of DBO **1** was carried out as displayed in Scheme 1. First, Suzuki coupling of 4-dodecyl-2-(trimethylsilylethynyl)phenylboronic acid (**2**) and 7-bromo-2-naphthaldehyde (**3**) gave 7-(4-dodecyl-2-(trimethylsilylethynyl)phenyl)-2-naphthaldehyde (**4**) in 97% yield. Then CuCl-mediated Glaser coupling of **4** provided diaryldiacetylene **5** in 98% yield. Subsequently, the key intermediate, bischrysene dialdehyde **6** was obtained through a $PtCl_2$-catalysed cycloaromatization in 48% yield. Direct cyclodehydrogenation of dialdehyde **6** to **9** under various Scholl conditions failed, most probably because of the strong electron withdrawing properties of the two aldehyde groups. Therefore, compound **6** was reduced with $NaBH_4$ and then protected with acetyl groups to obtain **7** in 86% yield over two steps. Notably, the oxidative cyclodehydrogenation of **7** succeeded with 2,3-dichloro-5,6-dicyano-1,4-benzoquinone (DDQ)/trifluoromethanesulfonic acid (CF_3SO_3H) at a low temperature (–78 °C), providing cove-edged graphene molecule **8** in 33% yield. The low temperature was crucial for this conversion, and no product was obtained when the reaction was carried out at 0 °C. The ester groups of **8** were then transformed to dialdehyde groups through a

hydrolysis/oxidation sequence in 70% yield. To convert the cove edges of **9** into zigzag edges, **9** was treated with mesitylmagnesium bromide to give a diol intermediate, which reacted with BF_3•OEt_2 under air to afford the target DBO **1** as a blue solid in 24% yield. The structure of DBO **1** was unambiguously proven by spectroscopic analysis. Fig. 1a displays the MALDI-TOF MS spectrum of **1** with an intense signal at *m/z* = 1044.66 Da, consistent with the expected molecular mass of 1044.66 Da. The experimental isotopic distribution was in good agreement with the calculated spectrum based on the chemical composition of $C_{80}H_{84}$. A well-resolved ^{1}H NMR spectrum of DBO **1** could be recorded in toluene-d_8 at 100 °C (Fig. 1b), and all the proton signals could be assigned with the assistance of 2D NMR spectroscopy (see SI).

The electrochemical property of DBO **1** was studied by cyclic voltammetry (CV) in a dichloromethane solution with ferrocene as an external standard (Fig. S2). Two reversible oxidation and reduction waves were observed, indicating the stability of these redox species. The HOMO and LUMO energy levels were estimated to be –4.84 eV and –3.22 eV, based on the onset oxidation and reduction potentials, respectively, with the electrochemical HOMO-LUMO gap of 1.62 eV.

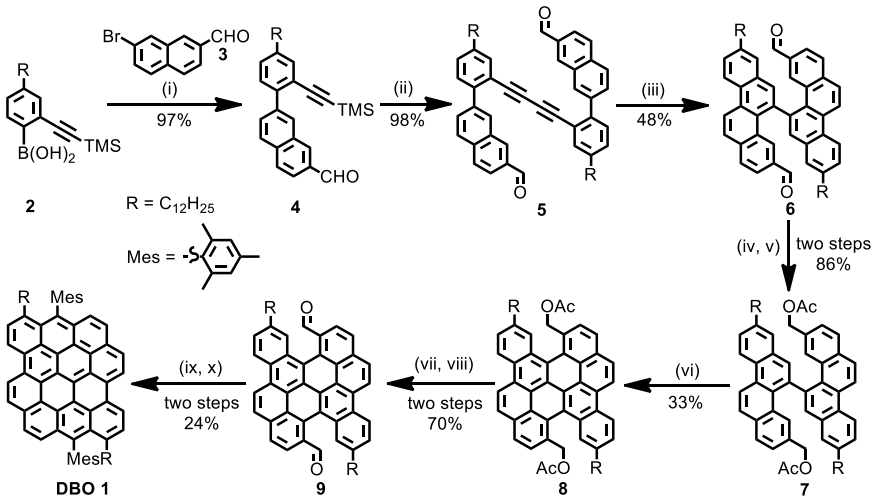

Scheme 1. Reaction conditions: (i) $Pd(PPh_3)_4$ (0.1 eq.), Na_2CO_3 (6.0 eq.), toluene/EtOH/H_2O = 4:1:1, 80 °C, 6 h; (ii) CuCl (1.0 eq.), DMF, 80 °C, 12 h, under air; (iii) $PtCl_2$ (0.3 eq.), toluene, 80 °C, 48 h; (iv) $NaBH_4$ (4.0 eq.), THF/MeOH = 2:1, r.t., 2 h; (v) Acetic anhydride, TEA (3.0 eq.), DMAP (0.3 eq.), DCM, r.t., 2 h; (vi) DDQ (4.0 eq.), DCM/CF_3SO_3H = 20:1, –78 °C, 2 h; (vii) KOH, THF/EtOH/H_2O, 80 °C, 12 h; (viii) PCC (2.0 eq.), DCM, r.t., 2 h; (ix) MesMgBr (20.0 eq.), THF, r.t. 2 h; (x) BF_3·OEt_2, DCM, r.t., 2 h, under air. DMF: dimethylformamide; THF: tetrahydrofuran; TEA: triethylamine; DMAP: 4-dimethylaminopyridine; DCM: dichloromethane; PCC: pyridinium chlorochromate.

The UV-*vis* absorption spectrum of DBO **1** in a toluene solution showed a maximum at 625 nm with a large absorption coefficient of $1.83 \times 10^5\ M^{-1}cm^{-1}$ (Fig. 2a). This absorption band could be assigned to HOMO→LUMO transition based on time-dependent density functional theory (TD-DFT) calculations at the B3LYP/6-311G(d,p) level (see Fig. S1 and Table S1). In comparison to the spectrum of precursor **9**, the low-energy absorption band was red-shifted by 88 nm due to the formation of zigzag edges and extension of aromatic core. The optical gap decreased from 2.19 eV to 1.93 eV upon the conversion of 9 into 1, according to the onsets of their UV-vis absorption spectra. The emission spectra of 9 and 1 in toluene solutions displayed maxima at 561 and 637 nm, with small Stokes shifts of 23 and 12 nm, respectively, indicating the rigid structures of these two molecules. Interestingly, the emission of 1 could be observed already under room light excitation (Fig. 2b), which is a clear signature of its strong emission properties. The absolute PLQY amounts to 79% (average value = 66.9% with a standard deviation of 6.6% over 35 measurements). To the best of our knowledge, this is one of the highest values reported for graphene molecules[14]. These promising photophysical features highlight the important role of the zigzag edges in DBO 1, significantly lowering the optical gap of 9 and realizing highly efficient red light emission.

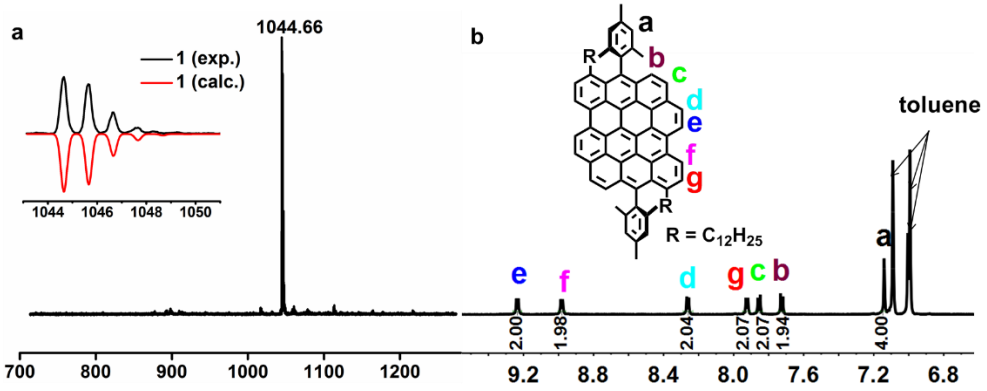

Figure 1. a) MALDI-TOF mass spectrum of DBO **1**; Inset shows a comparison between the calculated and experimental isotopic distributions; b) Aromatic region of the ^{1}H NMR spectrum of DBO **1**, recorded in toluene-d_8 at 100 °C (700 MHz).

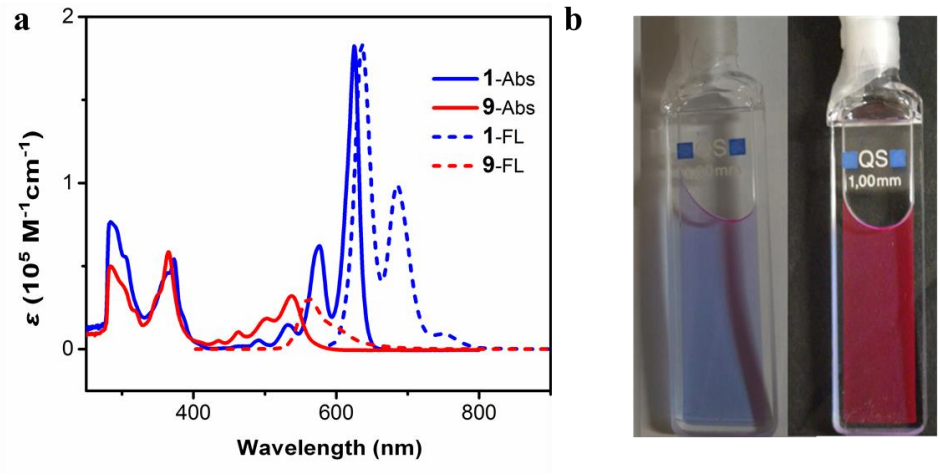

Figure 2. a) UV−*vis* absorption and fluorescence spectra of precursor **9** and DBO **1** (10^{-5} M in toluene for all measurements). b) Photographs of a toluene solution of DBO **1** with (right) and without (left) a black background, showing the red luminescence under room light.

The high PLQY, sharp absorption and emission peaks and small Stokes shift observed for DBO **1** prompted us to gain a deeper insight into its photophysics[15]. We carried out broadband (375-800 nm) TA measurements by using a pump pulse of 625 nm that is in resonance with the HOMO→LUMO transition.. The transient spectrum of DBO **1** (Fig. 3) displays four features, namely: (i) a negative signal centred at 450 nm that can be interpreted as a photoinduced absorption (PA) from the first excited state S_1 to higher excited states S_i; (ii) a positive signal at 650 nm that can be assigned to the depletion of the ground state due to the main HOMO→LUMO transition (photobleaching, PB); (iii) another positive PB signal centred at 570 nm, corresponding to its vibronic replica and (iv) a positive signal at 695 nm. The latter is a sign of stimulated emission given that: i) it is not present in the steady state absorption and ii) is red-shifted with respect to the main HOMO→LUMO transition peak[15a]. Although the origin of the SE signal in such graphene molecule is currently under investigation, we suppose it is related to vibronic relaxation within the higher-lying electronic excited state.

Stimulated emission signals are of great interest for acquiring direct information about possible optical gain properties of the material. Thus, we focus the discussion mainly on the SE signal and report the complete transient spectra and time-dynamics (up to 1 ns) data sets in the supplementary information. From the transient spectra of DBO **1** in toluene solution (Fig. 3a, top graph) the degree of decay is relatively low for all the signals (Fig. S3a-b). This is indicative of stable excited states

that can sustain stimulated emission and can also explain the high PLQY[16]. In addition, the sharp rise of all the transient signals, along with their linear dependence on pump fluence (see Fig. S3c-d), suggest that the photoexcitation mechanism is direct and does not involve any non-linear process.

For comparison, we have also performed ultrafast TA studies of soluble hexa-*peri*-hexabenzocoronene (HBC) derivative[17], which has solely the armchair edge structure, in toluene solution. The preliminary data (Fig. S4) show that all the transient features are incorporated in a large photoinduced absorption signal even at lower concentrations (down to 0.01 mg/mL). Furthermore, we could not observe any clear SE signal in the probed region (from 430 nm to 650 nm) for this HBC derivative, pointing to the uniqueness of the SE observed for DBO **1** and implying an important role of the zigzag edge for achieving the optical gain properties in graphene molecules.

We next turn to the characterisation of DBO **1** in thin film, which is essential for device applications (Fig. 3a, central graph). It appears that the transient peaks are broader than those in solution (e.g., for the PB signal: $FWHM_{solution}$ = 19.4 ± 0.4 nm; $FWHM_{film}$ = 34.3 ± 0.9 nm), and all the transient signal intensities decrease considerably in ≈ 200 fs (Fig. S5a-b). Thereby, the SE peak is overwhelmed by a negative PA feature in a time-frame that is comparable with the instrumental resolution (Fig. 3b). The broadening of the peaks points toward the aggregation of graphene molecules in films[6a]. The latter effect can be indicative of ultrafast and non-radiative intermolecular charge transfer processes in the solid state, which are promoted by the effective supramolecular packing occurring in such planar molecules[18], resulting in complete quenching of the PL in films.

To exploit gain properties of the material and possibly employ these features in solid-state devices, we embedded DBO **1** into a polystyrene (PS) matrix by simply mixing their solutions in toluene with 10, 5, 3 and 1 w% ratios. Such dilution approach has been used to inhibit intermolecular charge-transfer processes, and thus enhance SE signals[18a, 19] and ASE/LASER action in luminescent conjugated polymers[20]. Notably, this method works effectively also for graphene molecules, as blending allows one to extend the SE signal of DBO **1** for about ≈ 70 ps in the 1 w% **1**:PS blend (Fig.

3b; see Fig. S6a-h for the spectra and dynamics of all the DBO **1**:PS weight ratios). Moreover, the PS blending permits recovery of the emission of DBO **1** in the solid state, and a photoluminescence from the 1 w% DBO **1**:PS composite film can be detected upon UV-light exposure at 365 nm (Fig. 3c). It is worth noting that by diluting the graphene molecule DBO **1** in the PS matrix, the transient spectral features start resembling those observed in solution, with a progressive narrowing of the PB peaks, and a suppression of the PA signal (Fig. 3a and Fig. S6). All these spectroscopic findings point toward the occurrence of excitations with charge-transfer character, as it has been reported for luminescent conjugated polymers[15a, 18a, 19, 21]. In particular, both PA bands at 450 nm and 750 nm seem to stem from the photoinduced excitations of charges possibly originated upon intermolecular transfer, as their intensities decrease in solution and in blends with PS.

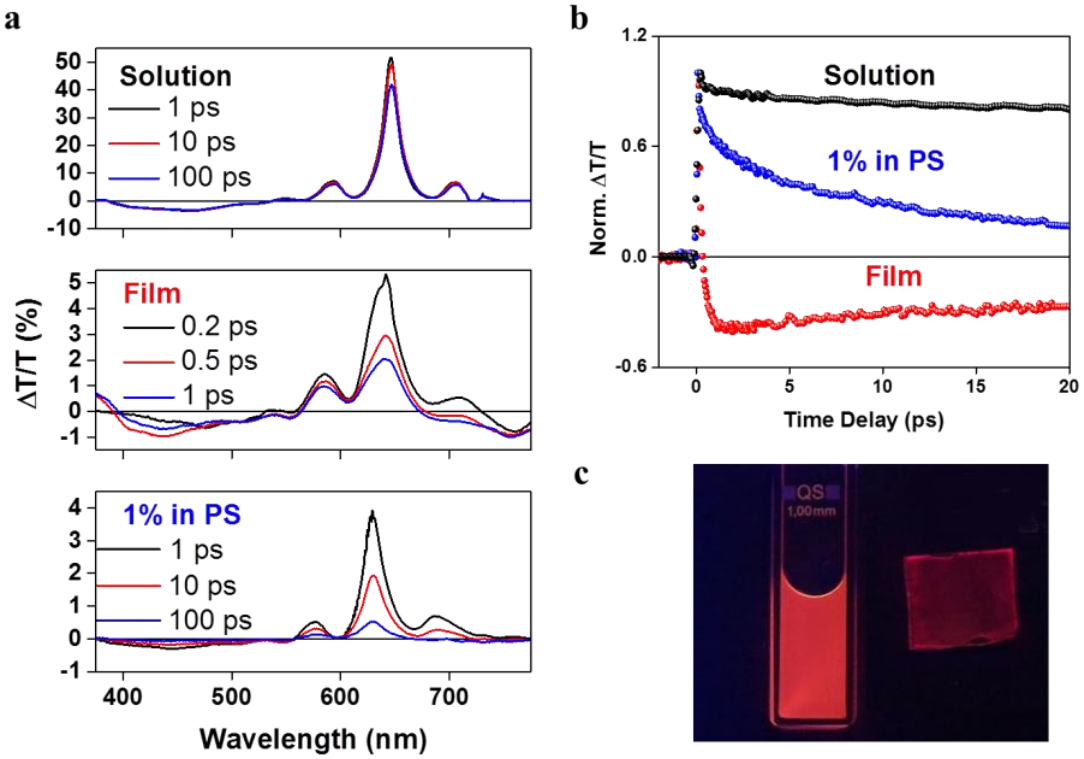

Figure 3. a) Ultrafast transient spectra of DBO **1** in solution (0.05 mg/mL in toluene), film and 1 w% blend with PS (deposited on fused silica substrates by drop-casting); b) Normalised time-decay dynamics for the SE emission signal (probe at 695 nm) for solution, film and 1 w% blend with PS. The spectra and time-decay dynamics shown above were taken with a pump fluence of ≈ 50 μJ cm^{-2}; c) Comparison of the luminescence of DBO **1** in solution and 1 w% PS composite film under UV irradiation at 365 nm.

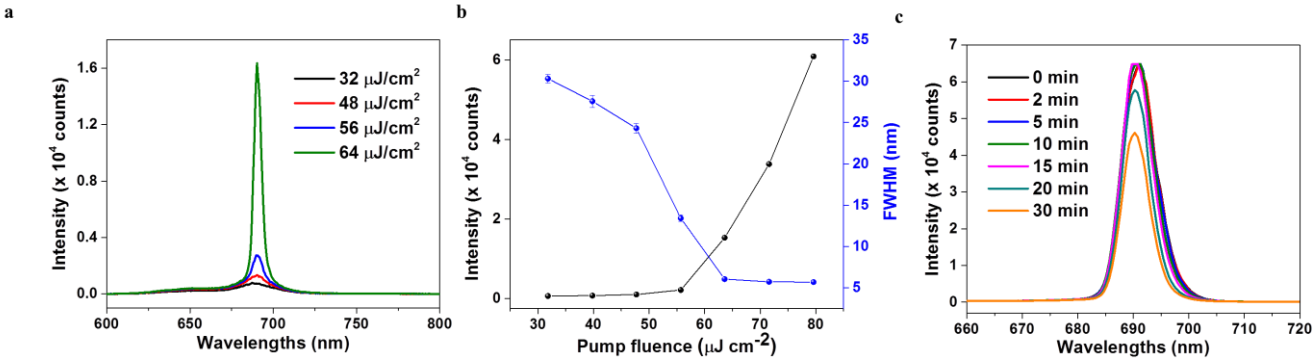

Figure 4. a) Photoluminescence spectra taken at laser power fluences below and above the ASE threshold; b) input-output characteristics of ASE action for the 1 w% blend in PS; c) evolution of the ASE signal over time taken at a laser pump fluence 5 times higher than the ASE threshold (320 μJ cm^{-2}).

Remarkably, the 1 w% DBO **1**:PS blend demonstrates amplified stimulated emission (ASE) action triggered above a relatively low laser fluence of 60 μJ cm^{-2} (Fig. 4a-b). Although PL line narrowing is observed also in the 3 w% blend (Fig. S7a-b), the laser power needed for FWHM narrowing is higher than the one required for the 1 w% blend (≈ 150 μJ cm^{-2}). This suggests that the 1 w% blend can minimize the intermolecular cross talking (in terms of charge transfer) that is crucial for avoiding fast non-radiative deactivations, and promote ASE action. Although the 10 w% and 5 w% blends do not show any ASE action, they still allow to observe a PL signal (Fig. S7c-d). To test the stability of DBO **1** against photodegradation, the sample was irradiated under air at a laser fluence 5 times higher than the ASE threshold (320 μJ cm^{-2}), yielding only a 30% decay after 30 minutes of intense irradiation (2 × 10^6 pulses). Although DBO **1** : PS blend films were stored under air, the same ASE emission was observed at least for 6 months after the preparation. The remarkable stability of DBO **1** against air, moisture and photodegradation must be ascribed to, both, the intrinsic robustness of its excited states, and to its incorporation into the inert PS matrix.

In summary, we have successfully synthesized DBO **1** as a novel graphene molecule with a unique combination of armchair and zigzag edges, demonstrating a low energy gap and strong red emission with remarkable PLQY of 79% as well as promising optical gain properties with low ASE threshold (≈ 60 μJ cm^{-2}) and high photochemical stability. With good solubility and thus enhanced

processability, DBO **1** holds great potential for future applications in low-cost organic devices, such as LASERs and OLEDs. Moreover, this study demonstrates the promise of graphene molecules with zigzag edges as stable and highly luminescent materials with optical gain properties. Further variety of such graphene molecules are presently synthesized in our laboratories and studied in view of their role as optical gain materials.

Acknowledgements

We thank the financial support from Graphene Flagship, the Max Planck Society, the European Union Project MoQuaS, and the EU Horizon 2020 Research and Innovation Programme under Grant Agreement N. 643238 (SYNCHRONICS) and N. 642196 (iSwitch). X.-Y. W. is grateful for the fellowship from Alexander von Humboldt Foundation.

Keywords: *graphene molecule• zigzag edges • transient absorption • stimulated emission • amplified spontaneous emission*

[1] a) I. D. Samuel, G. A. Turnbull, *Chem. Rev.* **2007**, *107*, 1272-1295; b) A. J. Kuehne, M. C. Gather, *Chem. Rev.* **2016**, *116*, 12823–12864; c) W. Zhang, J. Yao, Y. S. Zhao, *Acc. Chem. Res.* **2016**, *49*, 1691–1700; d) C. Kallinger, M. Hilmer, A. Haugeneder, M. Perner, W. Spirkl, U. Lemmer, J. Feldmann, U. Scherf, K. Müllen, A. Gombert, V. Wittwer, *Adv. Mater.* **1998**, *10*, 920-923; eN. Tessler, *Adv.Mater.* **1999**, *11*, 363-370.

[2] S. R. Forrest, *Nature* **2004**, *428*, 911-918.

[3] a) A. Narita, X. Feng, Y. Hernandez, S. A. Jensen, M. Bonn, H. Yang, I. A. Verzhbitskiy, C. Casiraghi, M. R. Hansen, A. H. Koch, G. Fytas, O. Ivasenko, B. Li, K. S. Mali, T. Balandina, S. Mahesh, S. De Feyter, K. Mullen, *Nat. Chem.* **2014**, *6*, 126-132; b) Y. W. Son, M. L. Cohen, S. G. Louie, *Nature* **2006**, *444*, 347-349.

[4] a) B. Trauzettel, D. V. Bulaev, D. Loss, G. Burkard, *Nat. Phys.* **2007**, *3*, 192-196; b) L. Cao, M. J. Meziani, S. Sahu, Y. P. Sun, *Acc. Chem. Res.* **2013**, *46*, 171-180.

[5] a) A. Narita, X. Y. Wang, X. Feng, K. Müllen, *Chem. Soc. Rev.* **2015**, *44*, 6616-6643; b) L. J. Zhi, K. Müllen, *J. Mater. Chem.* **2008**, *18*, 1472-1484; c) Y. Segawa, H. Ito, K. Itami, *Nat. Rev. Materi.* **2016**, *1*, 15002.

[6] a) S. Zhu, L. Wang, B. Li, Y. Song, X. Zhao, G. Zhang, S. Zhang, S. Lu, J. Zhang, H. Wang, H. Sun, B. Yang, *Carbon* **2014**, *77*, 462-472; b) S. Zhu, Q. Meng, L. Wang, J. Zhang, Y. Song, H. Jin, K. Zhang, H. Sun, H. Wang, B. Yang, *Angew. Chem.* **2013**, *52*, 3953-3957.

[7] K. A. Ritter, J. W. Lyding, *Nat. Mater.* **2009**, *8*, 235-242.

[8] J. D. Cox, F. Javier Garcia de Abajo, *Nat. Commun.* **2014**, *5*, 5725.

[9] a) V. Gupta, N. Chaudhary, R. Srivastava, G. D. Sharma, R. Bhardwaj, S. Chand, *J. Am. Chem. Soc.* **2011**, *133*, 9960-9963; b) S. Osella, A. Narita, M. G. Schwab, Y. Hernandez, X. Feng, K. Mullen, D. Beljonne, *ACS Nano* **2012**, *6*, 5539-5548.

[10] G. Soavi, S. Dal Conte, C. Manzoni, D. Viola, A. Narita, Y. Hu, X. Feng, U. Hohenester, E. Molinari, D. Prezzi, K. Mullen, G. Cerullo, *Nat. Commun.* **2016**, *7*, 11010.

[11] a) X. Yang, X. Dou, A. Rouhanipour, L. Zhi, H. J. Rader, K. Müllen, *J. Am. Chem. Soc.* **2008**, *130*, 4216-4217; b) M. G. Schwab, A. Narita, Y. Hernandez, T. Balandina, K. S. Mali, S. De Feyter, X. Feng, K. Mullen, *J. Am. Chem. Soc.* **2012**, *134*, 18169-18172; c) M. El Gemayel, A. Narita, L. F. Dossel, R. S. Sundaram, A. Kiersnowski, W. Pisula, M. R. Hansen, A. C. Ferrari, E. Orgiu, X. Feng, K. Mullen, P. Samori, *Nanoscale* **2014**, *6*, 6301-6314.

[12] a) P. Ruffieux, S. Wang, B. Yang, C. Sanchez-Sanchez, J. Liu, T. Dienel, L. Talirz, P. Shinde, C. A. Pignedoli, D. Passerone, T. Dumslaff, X. Feng, K. Mullen, R. Fasel, *Nature* **2016**, *531*, 489-492; b) A. Konishi, Y. Hirao, K. Matsumoto, H. Kurata, R. Kishi, Y. Shigeta, M. Nakano, K. Tokunaga, K. Kamada, T. Kubo, *J. Am. Chem. Soc.* **2013**, *135*, 1430-1437.

[13] J. Liu, P. Ravat, M. Wagner, M. Baumgarten, X. Feng, K. Müllen, *Angew. Chem.* **2015**, *54*, 12442-12446.

[14] a) S. Seifert, K. Shoyama, D. Schmidt, F. Würthner, *Angew. Chem.* **2016**, *55*, 6390-6395; b) S. Müller, K. Müllen, *Chem. Commun.* **2005**, 4045-4046.

[15] a) J. Cabanillas-Gonzalez, G. Grancini, G. Lanzani, *Adv. Mater.* **2011**, *23*, 5468-5485; b) G. Cerullo, C. Manzoni, L. Luer, D. Polli, *Photochem. Photobiol. Sci.* **2007**, *6*, 135-144.

[16] J. R. Lakowicz, *Principles of fluorescence spectroscopy*, Springer Science & Business Media, **2013**.

[17] M. Kastler, W. Pisula, D. Wasserfallen, T. Pakula, K. Mullen, *J. Am. Chem. Soc.* **2005**, *127*, 4286-4296.

[18] a) M. Yan, L. J. Rothberg, E. W. Kwock, T. M. Miller, *Phys. Rev. Lett.* **1995**, *75*, 1992-1995; b) N. J. Turro, *Modern molecular photochemistry*, University science books, **1991**.

[19] T. Virgili, D. Marinotto, C. Manzoni, G. Cerullo, G. Lanzani, *Phys. Rev. Lett.* **2005**, *94*, 117402.

[20] M. Morales-Vidal, P. G. Boj, J. M. Villalvilla, J. A. Quintana, Q. Yan, N. T. Lin, X. Zhu, N. Ruangsupapichat, J. Casado, H. Tsuji, E. Nakamura, M. A. Diaz-Garcia, *Nat. Commun.* **2015**, *6*, 8458.

[21] T. Virgili, D. Marinotto, G. Lanzani, D. D. C. Bradley, *Appl. Phys. Lett.* **2005**, *86*, 91113.

Supplementary Information

Synthesis of Dibenzo[hi,st]ovalene and Its Amplified Spontaneous Emission in a Polystyrene Matrix

Giuseppe M. Paternò*‡,[a] Qiang Chen*‡,[b] Xiao-Ye Wang,[b] Junzhi Liu,[c] Silvia G. Motti,[a] Annamaria Petrozza,[a] Xinliang Feng,[c] Guglielmo Lanzani,[a,d] Klaus Müllen*,[b] Akimitsu Narita*[b] and Francesco Scotognella*[a,d]

Table of Content

1. General experimental details

All reactions working with air- or moisture-sensitive compounds were carried out under argon atmosphere using standard Schlenk line techniques. Unless otherwise noted, all starting materials were purchased from commercial sources and used without further purification. All other reagents were used as received. Thin layer chromatography (TLC) was done on silica gel coated aluminum sheets with F254 indicator and preparative chromatographic separation was performed with silica gel (particle size 0.063-0.200 mm). Nuclear Magnetic Resonance (NMR) spectra were recorded using Bruker DPX 250, Bruker DPX 300, and Bruker DRX 700 MHz NMR spectrometers. Chemical shifts (δ) are expressed in ppm relative to the residual of solvent. Coupling constants (J) were recorded in Hertz. Field desorption mass (FD-MS) spectra were measured using a VG instruments ZAB 2-SE-FPD using 8 kV accelerating voltage. High-resolution mass spectra (HRMS) were recorded on a Bruker Reflex II-TOF spectrometer by matrix-assisted laser decomposition/ionization (MALDI) using 7,7,8,8-tetracyanoquinodimethane (TCNQ) as matrix.

1.1 UV-VIS absorption

UV-vis absorption spectra were recorded on a Perkin-Elmer Lambda 900 spectrometer at room temperature using a 10 mm quartz cell. Photoluminescence spectra were recorded on a J&MTIDAS spectrofluorometer.

1.2 Cyclic voltammetry

Cyclic voltammetry (CV) measurements were performed on a GSTAT-12 in a three-electrode cell in dichloromethane solution of n-Bu_4NPF_6 (0.1 M) at a scan rate of 50 mV/s at room temperature. A silver wire, a Pt wire and a glassy carbon electrode were used as the reference electrode, the counter electrode, and the working electrode, respectively.

1.3 Ultrafast Transient Absorption

For the non-degenerate pump and probe measurements, the molecule was dissolved in toluene with a concentration of 0.05 mg mL^{-1}. Such concentration value was optimized to give an absorbance of ~1 in a 1 mm thick cuvette. Neat films of the molecule were produced via drop-casting deposition on fused silica substrates. For DBO 1: polystyrene solid blends, we dissolved the polystyrene (PS, Aldrich, Mw = 200,000) and the DBO 1 in toluene with a concentration of 10 mg/mL, and then we mixed the two molecules together, with DBO 1 : PS weight ratios of 10%, 5%, 3% and 1%. We employed an amplified Ti:sapphire laser with 2 mJ output energy, 1 kHz repetition rate and a central energy of 1.59 eV (800 nm). We used a pump wavelength of 620 nm excitation, which is resonant with the main $\pi \rightarrow \pi^*$ transition. Such pump pulses were generated by using a visible optical parameter amplifier (OPA). Pump pulses were focused on a 200 μm spot (diameter), keeping pump fluences at ~ 50 μJ cm-2. As a probe pulse, we used a broadband white light super-continuum generated in CaF_2 in the spectral region from 340 nm to 800 nm.

1.4 ASE and PLQY

For ASE measurements, the blend was spin-cast onto a glass substrate with a spin speed of 1000 rotations per minute yielding a thickness of ≈ 400 nm, as measured by profilometer. ASE characterisations were performed by using an amplified Ti:sapphire laser with 2 mJ output energy and 2 kHz repetition rate at 625 nm. We used a 7.5 cm cylindrical focal lens to focus the pump beam into a 2 mm × 0.1 mm strip and collected the emission from the edge of the film with a fibre spectrometer (resolution 0.5 nm).

For absolute PLQY measurements, we pumped with a CW diode laser (Oxxius 561 nm) at 560 nm. The sample was placed in the centre of an integration sphere and the pump beam was directed on it unfocused. Signal was collected in a fibre coupled into a spectrometer (Ocean Optics Maya Pro 2000). The system response was corrected by measuring a calibrated tungsten lamp and the PLQY was calculated according to the methods described in reference De Mello et al., *Adv. Mater.* **9**, 230-232 (1997).

2. Synthetic details

Synthesis of 4-dodecyl-2-(trimethylsilylethynyl)phenylboronic acid (**2**):

The synthesis of 4-dodecyl-2-(trimethylsilylethynyl)phenylboronic acid (**2**) is shown in Scheme S1. 4-Dodecyl-2-iodoaniline (**S2**) was prepared by iodination of 4-dodecylaniline (**S1**) with iodine in toluene, followed by Sandmeyer bromination to afford **S3** in 78% yield. Subsequently, Sonogashira coupling of **S3** with trimethylsilyl acetylene gave **S4** in 96% yield, followed by borylation with *n*-BuLi/triisopropyl borate and hydrolysis to give **2** in 94% yield.

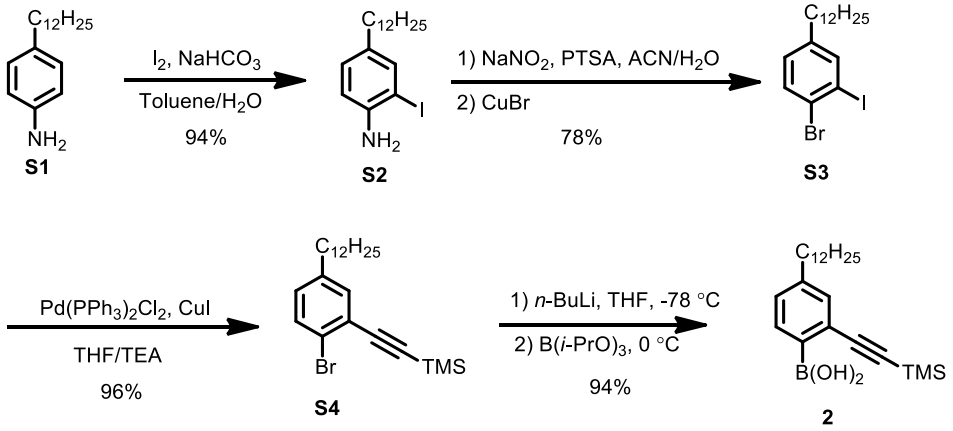

Scheme S1. Synthetic route to compound **2**.

Synthesis of 4-dodecyl-2-iodoaniline (**S2**)

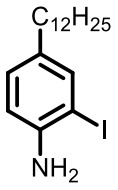

To a solution of 4-dodecylaniline (10.00 g, 38.25 mmol) and $NaHCO_3$ (4.82 g, 57.4 mmol) in toluene (80 mL) and water (9 mL) was added iodine (10.7 g, 42.1 mmol) in portions. The obtained mixture was stirred at room temperature overnight. Saturated $Na_2S_2O_3$ aqueous solution (50 mL) was added

to quench the reaction and stirred for another 0.5 h. The organic phase was separated and the aqueous solution was extracted with ethyl acetate (EA) (50 mL) for 3 times, the combined organic layers were washed with brine (50 mL) and dried over Na_2SO_4. The solvents were evaporated under reduced pressure and the residue was purified by column chromatography over silica gel (eluent: *n*-hexane/EA = 10 : 1) to give compound **S2** (14.0 g, 94% yield) as a white solid. TLC R_f = 0.5 (*n*-hexane/EA = 10 : 1); ^{1}H NMR (250 MHz, $CDCl_3$, 25 °C, ppm) δ 7.47 (d, J = 1.9 Hz, 1H), 6.96 (dd, J = 8.1, 2.0 Hz, 1H), 6.73 (d, J = 8.1 Hz, 1H), 2.45 (t, J = 7.4 Hz, 2H), 1.61 − 1.43 (m, 2H), 1.37 − 1.01 (m, 18H), 0.88 (t, J = 6.3 Hz, 3H); ^{13}C NMR (62.5 MHz, $CDCl_3$, 25 °C, ppm) δ 144.1, 138.6, 135.4, 129.6, 115.1, 84.8, 34.7, 32.1, 31.8, 29.8, 29.8, 29.7, 29.6, 29.5, 29.3, 22.9, 14.3; FD-MS (8 kV): *m/z* 388.8; HRMS (ESI): *m/z* Calcd for $C_{18}H_{30}IN$: 388.1496 $[M + H]^+$, found: 388.1515.

Synthesis of 4-bromo-3-iododododecylbenzene (**S3**)

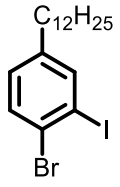

S3

A 500 mL round bottom flask was charged with 4-dodecyl-2-iodoaniline (**S2**) (6.00 g, 16.0 mmol), *p*-toluenesulfonic acid monohydrate (8.80 g, 47.0 mmol) and acetonitrile (200 mL). To the suspension was added slowly at 0 °C a solution of $NaNO_2$ (2.10 g, 31.0 mmol) in water (12 mL) over 0.5 h and then the mixture was stirred for another 2 h. Subsequently, CuBr (5.60 g, 39.0 mmol) was added in one portion. After stirring at 0 °C for another 1 h, the mixture was gradually warmed up to r.t. and then heated at 60 °C for 0.5 h. After cooling down to r.t., the mixture was diluted with EA (200 mL), and washed with water (150 mL). The organic phase was separated and washed with brine (100 mL), dried over Na_2SO_4 and concentrated. The obtained residue was purified by column chromatography over silica gel (eluent: *n*-hexane) to give compound **S3** (5.50 g, 78% yield) as colorless oil. TLC R_f = 0.9 (*n*-hexane); ^{1}H NMR (250 MHz, CD_2Cl_2, 25 °C, ppm) δ 7.71 (d, J = 2.0 Hz, 1H), 7.51 (d, J = 8.2

Hz, 1H), 7.04 (dd, J = 8.2, 2.1 Hz, 1H), 2.51 (t, J = 3.6 Hz, 2H), 1.65 – 1.45 (m, 2H), 1.28 (m, 18H), 0.88 (t, J = 6.5 Hz, 3H); ^{13}C NMR (62.5 MHz, CD_2Cl_2, 25 °C, ppm) δ 144.5, 140.6, 132.6, 130.3, 126.5, 101.1, 35.2, 32.3, 31.5, 30.1, 30.1, 30.0, 29.8, 29.7, 29.5, 23.1, 14.3; FD-MS (8 kV): *m/z* 451.4; HRMS (MALDI-TOF): *m/z* Calcd for $C_{18}H_{28}BrI$: 450.0414 $[M]^+$, found: 450.0366.

Synthesis of 4-bromo-3-[(trimethylsilyl)ethynyl]dodecylbenzene (**S4**)

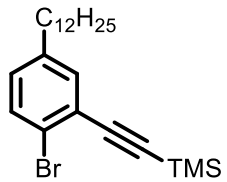

S4

To a degassed solution of 4-bromo-3-iododododecylbenzene (**S3**) (5.50 g, 12.0 mmol) in THF (34 mL) and triethylamine (34 mL) was added $PdCl_2(PPh_3)_2$ (170 mg, 0.240 mmol) and CuI (93.0 mg, 0.480 mmol). The resulting mixture was bubbled with Ar for 10 min, and then (trimethylsilyl)acetylene (1.30 g, 13.4 mmol) was added via a syringe. After stirring at room temperature overnight, the reaction mixture was diluted with EA (200 mL), washed with water (150 mL) and brine (100 mL) and dried over Na_2SO_4. The solvent was removed under reduced pressure and the residue was purified by column chromatography over silica gel (eluent: *n*-hexane) to give compound **S3** (4.90 g, 96% yield) as colorless oil. TLC R_f = 0.8 (*n*-hexane/EA = 1 : 0); ^{1}H NMR (250 MHz, CD_2Cl_2, 25 °C, ppm) δ 7.46 (d, J = 8.2 Hz, 1H), 7.32 (d, J = 2.1 Hz, 2H), 7.01 (dd, J = 8.3, 2.3 Hz, 1H), 2.52 (t, J = 8.0 Hz, 2H), 1.66 – 1.50 (m, 2H), 1.36 – 1.22 (m, 18H), 0.87 (t, J = 6.8 Hz, 3H), 0.27 (s, 9H); ^{13}C NMR (62.5 MHz, CD_2Cl_2, 25 °C, ppm) δ 142.7, 134.0, 132.5, 130.6, 125.1, 122.6, 103.6, 99.3, 35.4, 32.4, 31.5, 30.1, 30.1, 29.9, 29.8, 29.7, 29.5, 23.1, 14.3, 0.1; FD-MS (8 kV): *m/z* 420.8.

Synthesis of (4-dodecyl-2-((trimethylsilyl)ethynyl)phenyl)boronic acid (**2**)

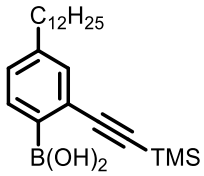

2

To a solution of 4-bromo-3-[(trimethylsilyl)ethynyl]dodecylbenzene (**S4**) (4.90 g, 12.0 mmol) in THF (60 mL) was added dropwise *n*-BuLi (8.7 mL, 1.6 M in hexane) at –78 °C. After stirring at this temperature for 1 h, triisopropyl borate (4.40 g, 23.0 mmol) was added *via* a syringe. The mixture was gradually warmed to room temperature and stirred for 16 h. The reaction was quenched by adding 1 N HCl (36 mL) and stirred at room temperature for 0.5 h. The mixture was extracted with EA (50 mL) for 3 times. The organic layers were combined, washed with brine (100 mL) and dried over Na_2SO_4. The solvents were evaporated under reduced pressure and the obtained residue was purified by column chromatography over silica gel (*n*-hexane/EA = 10 : 1) to give compound **2** (4.20 g, 94% yield) as a white solid. TLC R_f = 0.2 (*n*-hexane/EA = 10 : 1); ^{1}H NMR (250 MHz, CD_2Cl_2, 25 °C, ppm) δ 7.84 (d, J = 7.8 Hz, 1H), 7.34 (d, J = 1.7 Hz, 1H), 7.22 (dd, J = 7.8, 1.7 Hz, 2H), 5.79 (s, 2H), 2.60 (t, J = 7.5 Hz, 2H), 1.70-1.56 (m, 2H), 1.40 – 1.20 (m, 18H), 0.88 (t, J = 6.8 Hz, 3H), 0.29 (s, 9H); ^{13}C NMR (62.5 MHz, CD_2Cl_2, 25 °C, ppm) δ 146.8, 136.1, 133.2, 129.6, 127.1, 107.3, 98.9, 36.2, 32.5, 31.7, 30.3, 30.3, 30.2, 30.1, 29.9, 29.8, 23.1, 14.3, 0.0; FD-MS (8 kV): *m/z* 387.0.

Synthesis of 2-bromo-7-aldehydenaphthalene (**3**)

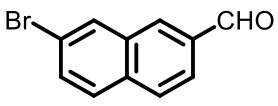

3

To a THF (28 mL) solution of 2,7-dibromonaphthalene (2.00 g, 7.00 mmol) was added dropwise *n*-BuLi (4.8 mL, 1.6 M in *n*-hexane) at –78 °C. After stirring for 0.5 h, anhydrous dimethylformamide (DMF) (660 mg, 9.10 mmol) was added via a syringe and the solution was stirred for another 0.5 h

at this temperature. Then the mixture was slowly warmed up to room temperature over 1 h. After stirring at room temperature for 1 h, water (20 mL) was added to quench the reaction. THF phase was separated and the aqueous phase was extracted with EA (30 mL) for 3 times. The combined organic layers were washed with brine (50 mL) and dried over Na_2SO_4. The solvent was evaporated under reduced pressure and the residue was purified by column chromatography over silica gel (*n*-hexane/EA = 15 : 1) to give compound **3** (1.30 g, 80% yield) as a white solid. TLC R_f = 0.3 (*n*-hexane/EA = 10 : 1); ^{1}H NMR (250 MHz, CD_2Cl_2, 25 °C, ppm) δ 10.15 (s, 1H), 8.27 (d, J = 1.1 Hz, 1H), 8.21 (d, J = 1.8 Hz, 1H), 7.95 (d, J = 1.1 Hz, 2H), 7.83 (d, J = 7.5 Hz, 1H), 7.73 (dd, J = 8.8, 1.9 Hz, 1H); ^{13}C NMR (62.5 MHz, CD_2Cl_2, 25 °C, ppm) δ 192.1, 135.4, 135.2, 134.2, 133.4, 132.6, 131.8, 130.1, 129.5, 123.6, 121.4; FD-MS (8 kV): *m/z* 234.5; HRMS (MALDI-TOF): *m/z* Calcd for $C_{11}H_7BrO$: 233.9675 $[M]^+$, found: 233.9574.

Synthesis of 7-(4-dodecyl-2-(trimethylsilylethynyl)phenyl)-2-naphthaldehyde (**4**)

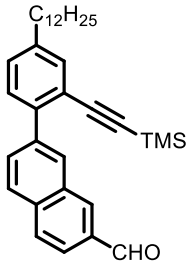

4

To a two-necked round bottom flask was added compound **2** (1.97 g, 5.10 mmol), compound **3** (1.21 g, 5.10 mmol) and Na_2CO_3 (3.25 g, 30.6 mmol). The flask was evacuated and backfilled with Ar for 3 times. Then toluene/EtOH/H_2O (128 mL/32 mL/32 mL) was added via a syringe. The mixture was degassed by bubbling with Ar for 15 minutes before $Pd(PPh_3)_4$ (320 mg, 0.300 mmol) was added. The mixture was heated at 80 °C for 6 h under Ar atmosphere. Then the reaction mixture was cooled down to r.t. and extracted with EA (30 mL) for 3 times. The combined organic layers were washed with brine (80 mL) and then dried over anhydrous Na_2SO_4. The solvents were removed under reduced pressure and the residue was purified by column chromatography (*n*-hexane/EA = 20 : 1) to give

compound **4** (2.45 g, 97% yield) as a white solid. TLC R_f = 0.5 (n-hexane/EA = 10 : 1); ^{1}H NMR (250 MHz, CD_2Cl_2, 25 °C, ppm) δ 10.11 (s, 1H), 8.31 (s, 1H), 8.20 (s, 1H), 7.96 – 7.80 (m, 4H), 7.43 – 7.29 (m, 2H), 7.20 (dd, *J* = 8.0, 1.9 Hz, 1H), 2.56 (t, *J* = 7.8 Hz, 2H), 1.66 – 1.49 (m, 2H), 1.34 – 1.12 (m, 18H), 0.79 (t, *J* = 6.8 Hz, 1H), 0.00 (s, 9H); ^{13}C NMR (62.5 MHz, CD_2Cl_2, 25 °C, ppm) δ 192.5, 143.2, 139.6, 136.0, 135.2, 135.0, 134.0, 133.0, 131.5, 130.1, 130.0, 129.8, 129.3, 127.9, 123.2, 105.4, 98.0, 35.9, 32.6, 31.9, 30.3, 30.2, 30.1, 30.0, 29.9, 23.3, 14.6, 0.0; FD-MS (8 kV): *m/z* 497.0; HRMS (MALDI-TOF): *m/z* Calcd for $C_{34}H_{44}OSi$: 496.3156 $[M]^+$, found: 496.3100.

Synthesis of 1,4-bis(2-(7-formylnaphthalen-2-yl)-5-dodecylphenyl)buta-1,3-diyne (**5**)

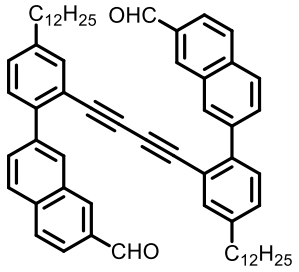

5

To a solution of compound **4** (1.60 g, 3.20 mmol) in DMF (24 mL) was added CuCl (320 mg, 3.20 mmol). The reaction mixture was heated at 80 °C under air. After 12 h, the reaction mixture was diluted with EA (100 mL) and washed with 1 N HCl (50 mL). The aqueous phase was then extracted with EA (30 mL) for 3 times. The combined organic layers were washed with saturated aqueous Na_2CO_3 (60 mL) and brine (60 mL) before drying over Na_2SO_4. The solvents were removed under reduced pressure and the residue was purified by column chromatography over silica gel (*n*-hexane/EA = 10 : 1) to give compound **5** (1.34 g, 98% yield) as a white solid. TLC R_f = 0.3 (*n*-hexane/EA = 10 : 1); ^{1}H NMR (250 MHz, CD_2Cl_2, 25 °C, ppm) δ 10.01 (s, 2H), 8.22 (s, 2H), 8.04 (s, 2H), 7.83 (d, *J* = 1.4 Hz, 4H), 7.76 (d, *J* = 1.5 Hz, 4H), 7.40 (d, *J* = 1.5 Hz, 2H), 7.33 (d, *J* = 7.9 Hz, 1H), 7.28 – 7.19 (m, 2H)), 2.56 (t, *J* = 7.5 Hz, 4H), 1.70 – 1.45 (m, 4H), 1.40 – 1.15 (m, 20H), 0.84 (t, *J* = 6.5 Hz, 6H); ^{13}C NMR (62.5 MHz, CD_2Cl_2, 25 °C, ppm) δ 192.5, 143.3, 141.9, 139.3, 136.0, 135.1, 135.0, 134.7, 133.1, 131.0, 130.7, 130.3, 129.9, 129.2, 128.1, 123.3, 120.3, 82.3, 76.87, 35.8,

32.5, 31.8, 30.3, 30.2, 30.1, 30.0, 29.8, 23.3, 14.5; FD-MS (8 kV): *m/z* 848.6; HRMS (MALDI-TOF): *m/z* Calcd for $C_{62}H_{70}O_2$: 846.5370 $[M]^+$, found: 846.5408.

Synthesis of 8,8'-didodecyl-[5,5'-bichrysene]-3,3'-dicarbaldehyde (**6**)

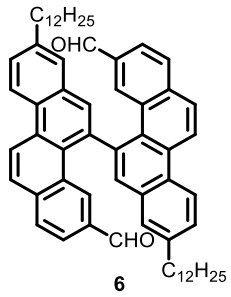

6

A Schlenk flask charged with compound **5** (630 mg, 0.744 mmol) and $PtCl_2$ (59.0 mg, 0.220 mmol) was dried under vacuum for 1 h and then was evacuated and backfilled with Ar for 3 times before anhydrous toluene (50 mL) was added via a syringe. The mixture was degassed by three freeze-pump-thaw cycles and heated at 85 °C for 48 h under Ar atmosphere. After confirming the completion of the reaction by ^{1}H NMR, the solvent was removed under reduced pressure and the residue was purified by column chromatography over silica gel (eluent: *n*-hexane/EA = 10 : 1) to give compound **6** (300 mg, 48% yield) as a white solid. TLC R_f = 0.3 (*n*-hexane/EA = 10 : 1); ^{1}H NMR (250 MHz, CD_2Cl_2, 25 °C, ppm) δ 9.02 (d, J = 9.3 Hz, 2H), 8.85 (d, J = 8.8 Hz, 2H), 8.69 (s, 2H), 8.20 (s, 2H), 8.00 (d, J = 7.7 Hz, 4H), 7.81 (d, J = 8.0 Hz, 4H), 7.72 (dd, J = 9.1 Hz, 1.4 Hz, 2H), 7.60 (dd, J = 8.2, 1.5 Hz, 2H), 2.89 (t, J = 7.7 Hz, 4H), 1.90 – 1.70 (m, 4H), 1.49 – 1.15 (m, 36H), 0.94 – 0.73 (m, 6H); ^{13}C NMR (62.5 MHz, CD_2Cl_2, 25 °C, ppm) δ 192.0, 143.2, 140.5, 136.7, 134.1, 133.2, 132.8, 131.5, 131.3, 130.5, 129.5, 129.4, 128.7, 128.3, 127.9, 127.6, 125.3, 123.7, 122.4, 36.3, 32.3, 31.7, 30.1, 30.0, 30.0, 29.9, 29.8, 29.7, 23.1, 14.3; FD-MS (8 kV): *m/z* 848.4; HRMS (MALDI-TOF): *m/z* Calcd for $C_{62}H_{70}O_2$: 869.5268 $[M + Na]^+$, found: 869.5292.

Synthesis of 3,3'-diacetoxymethyl-8,8'-didodecyl-5,5'-bichrysene (**7**)

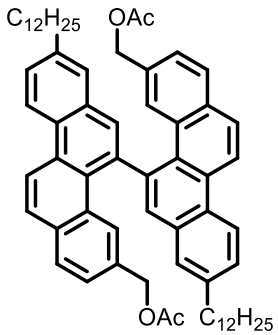

7

To a solution of compound **6** (200 mg, 0.230 mmol) in the mixture of THF (10 mL) and methanol (5 mL) was added $NaBH_4$ (71.0 mg, 1.90 mmol). The mixture was stirred at room temperature for 1 h. The completion of the reaction by confirmed by TLC analysis (*n*-hexane/EA = 4 : 1), and then acetone (5 mL) was added to quench the reaction. After stirring for another 10 minutes, the solvent was evaporated and the residue was dissolved in EA (50 mL). The organic solution was then washed with water (30 mL) and brine (30 mL), and dried over Na_2SO_4. The solvent was evaporated to give a diol intermediate (195 mg, 95% crude yield) as a white solid. The diol intermediate (150 mg, 177 μmol) was dissolved in anhydrous dichloromethane (DCM) (10 mL), and then triethylamine (54 mg, 0.53 mmol), 4-dimethylaminopyridine (6.5 mg, 53 μmol) and acetic anhydride (54 mg, 0.53 mmol) were added. The reaction mixture was stirred at room temperature for 2 h, and then TLC analysis (*n*-hexane/EA = 4 : 1) showed the reaction was completed. The solvent was evaporated and the residue was purified by column chromatography over silica gel (*n*-hexane/EA = 5 : 1) to give compound **7** (150 mg, 91% yield) as a white solid. TLC R_f = 0.5 (*n*-hexane/EA = 5 : 1); ^{1}H NMR (250 MHz, CD_2Cl_2, 25 °C, ppm) δ 8.84 (d, J = 9.2 Hz, 2H), 8.75 (d, J = 9.2 Hz, 2H), 8.05 – 7.95 (m, 4H), 7.80 (d, J = 8.2 Hz, 2H), 7.70 (s, 2H), 7.60 – 7.52 (m, 2H), 7.17 (dd, J = 8.2, 1.5 Hz, 2H), 4.45 – 4.28 (m, 4H), 2.73 (t, J = 7.9 Hz, 4H), 1.73 – 1.58 (m, 4H), 1.40 – 1.10 (m, 38H), 1.13 (s, 6H), 0.85 – 0.72 (m, 6H); ^{13}C NMR (62.5 MHz, CD_2Cl_2, 25 °C, ppm) δ 170.4, 142.5, 141.2, 133.3, 133.0, 132.5, 131.0, 130.9, 130.5, 128.7, 128.6, 128.3, 127.5, 127.4, 126.8, 125.4, 123.6, 122.2, 66.1, 36.2, 32.3, 31.8,

30.1, 30.0, 29.9, 29.9, 29.8, 29.7, 23.1, 20.0, 14.3; FD-MS (8 kV): *m/z* 935.7; HRMS (MALDI-TOF): *m/z* Calcd for $C_{66}H_{78}O_4$: 934.5895 $[M]^+$, found: 934.5909.

Synthesis of 5,14-diacetoxymethyl-3,12-didodecylbenzo[*a*]dinaphtho[2,1, 8-*cde*:1',2',3',4'-*ghi*]perylene (**8**)

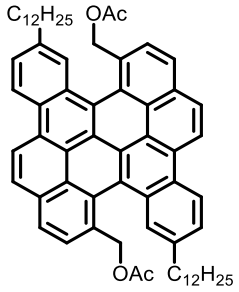

8

A solution of compound **7** (150 mg, 0.160 mmol) and DDQ (146 mg, 0.640 mmol) in anhydrous DCM (60 mL) was cooled down to –78 °C and stirred at this temperature for 10 min. To this vigorously stirred solution was added slowly trifluoromethanesulfonic acid (CF_3SO_3H) (3 mL) and the obtained mixture was stirred at –78 °C for another 2 h. Then the reaction was quenched by pouring into saturated aqueous Na_2CO_3. DCM phase was separated and the aqueous phase was extracted with DCM (30 mL) for 2 times. The combined organic layers were washed with brine (50 mL), and dried over Na_2SO_4. The solvents were evaporated and the residue was purified by column chromatography over silica gel (*n*-hexane/EA = 10 : 1) to give compound **8** (50 mg, yield 33%) as a yellow solid. TLC R_f = 0.3 (*n*-hexane/EA = 4 : 1); ^{1}H NMR (250 MHz, CD_2Cl_2, 25 °C, ppm) δ 8.86 (d, J = 9.1 Hz, 2H), 8.75 (d, J = 9.1 Hz, 2H), 8.10 – 7.89 (m, 2H), 7.80 (d, J = 8.2 Hz, 2H), 7.70 (s, 2H), 7.62 – 7.46 (m, 2H), 7.17 (d, J = 8.2, 2H), 4.49 – 4.18 (m, 4H), 2.74 (t, J = 7.8 Hz, 4H), 1.78 – 1.57 (m, 4H), 1.24 – 1.16 (m, 36H), 1.15 (s, 6H), 0.80 (t, J = 6.6 Hz, 6H). ^{13}C NMR (63 MHz, CD_2Cl_2, 25 °C, ppm) δ 170.8, 142.1, 133.0, 131.2, 130.3, 128.0, 127.9, 127.8, 127.6, 127.4, 127.1, 126.4, 126.2, 125.8, 123.9, 122.3, 122.1, 121.7, 66.6, 36.9, 32.5, 32.2, 30.2, 30.2, 30.2, 30.1, 29.9, 23.3, 21.1, 14.5 FD-MS (8KV): *m/z* 931.7; HRMS (MALDI-TOF): *m/z* Calcd for $C_{66}H_{74}O_4$: 930.5582 $[M]^+$, found: 930.5546.

Synthesis of 3,12-didodecyl-5,14-diformylbenzo[*a*]dinaphtho[2,1, 8-*cde*:1',2',3',4'-*ghi*]perylene (**9**)

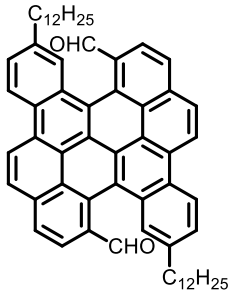

9

To a solution of compound **8** (30 mg, 32 μmol) in THF (9 mL) and ethanol (9 mL) was added 10% aqueous solution of KOH (3 mL). The mixture was stirred at reflux for 12 h. After cooling to r.t., the reaction mixture was diluted with EA (20 mL) and washed with water (10 mL), brine (10 mL) and then dried over Na_2SO_4. The solvent was evaporated and the obtained residue was dissolved in anhydrous DCM (20 mL). To the obtained solution was added pyridinium chlorochromate (PCC) (15 mg, 69 μmol) and then the reaction mixture was stirred at room temperature for 2 h. Methanol (1 mL) was added to quench the reaction and the mixture was stirred for another 10 min. The solvent was removed under reduced pressure and the residue was purified by column chromatography over silica gel (*n*-hexane/EA = 4 : 1) to give compound **9** (19 mg, 70% yield) as a red solid. ^{1}H NMR (250 MHz, CD_2Cl_2, 25 °C, ppm) δ 9.59 (s, 2H), 8.94 (d, J = 9.3 Hz, 2H), 8.71 (d, J = 8.8 Hz, 2H), 8.45 (d, J = 8.2 Hz, 2H), 8.36 (s, 2H), 8.31 (d, J = 5.9 Hz, 2H), 8.28 (d, J = 5.0 Hz, 2H), 7.55 – 7.45 (m, 2H), 2.68 (t, J = 7.9 Hz, 2H), 1.65 – 1.55 (m, 2H), 1.23 – 1.55 (s, 36H), 0.75 – 0.95 (m, 6H); ^{13}C NMR (62.5 MHz, CD_2Cl_2, 25 °C, ppm) δ 190.9, 143.6, 134.3, 132.7, 132.5, 131.4, 128.8, 128.6, 128.2, 127.6, 127.4, 125.9, 125.2, 124.9, 124.8, 124.5, 123.6, 121.8, 121.1, 36.9, 32.5, 32.2, 31.8, 30.3, 30.2, 30.1, 30.1, 29.9, 23.3, 23.2, 14.4 FD-MS (8 kV): *m/z* 843.7; HRMS (MALDI-TOF): *m/z* Calcd for $C_{66}H_{74}O_4$: 842.5063 $[M]^+$, found: 842.5070.

Synthesis of 5,13-didodecyl-6,14-dimesityldibenzo[*hi*,*st*]ovalene (**1**)

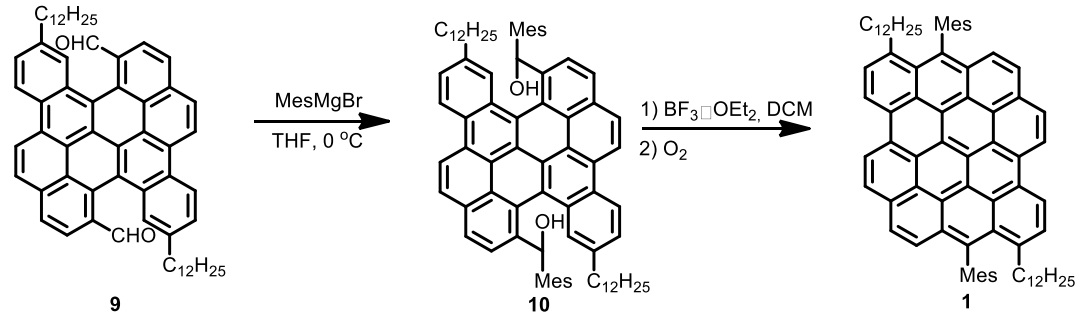

To compound **9** (40 mg, 47 μmol) dissolved in anhydrous THF (30 mL) was added mesitylmagnesium bromide (1.0 mL, 1.0 M in diethyl ether, 1.0 mmol) under Ar. The mixture was stirred at room temperature for 2 h, and then the solution was poured into water (20 mL) and extracted with EA (30 mL) for 3 times. The combined organic layers were washed with brine (30 mL) and dried over Na_2SO_4. After removing the solvents in vacuo the resulting crude product of compound **10** was dissolved in anhydrous DCM (10 mL) and $BF_3{\cdot}OEt_2$ (1.0 mL) was added. The mixture was stirred at room temperature for 2 h, and then quenched with saturated aqueous $NaHCO_3$ (10 mL). The organic phase was separated and dried over Na_2SO_4. The solvents were evaporated under reduced pressure and the residue was purified by column chromatography over silica gel (eluent: *n*-hexane/EA = 10 : 1) to give compound **1** (12 mg, 24% yield) as a blue solid. ^{1}H NMR (700 MHz, toluene-d_8, 100 °C, ppm) δ 9.23 (d, J = 8.5 Hz, 2H), 8.98 (d, J = 8.5 Hz, 2H), 8.26 (d, J = 7.9 Hz, 2H), 7.92 (d, J = 7.7 Hz, 2H), 7.85 (d, J = 9.4 Hz, 2H), 7.73 (d, J = 9.2 Hz, 2H), 7.14 (s, 4H), 2.88 (t, J = 8.4 Hz, 4H), 2.48 (s, 6H), 2.07 (s, 12H), 1.45 – 1.35 (m, 20H), 1.30 – 1.25 (m, 4H), 0.92 (t, J = 6.9 Hz, 6H). ^{13}C NMR (62.5 MHz, benzene-d_6, 25 °C, ppm) δ 141.1, 139.9, 137.9, 137.5, 134.9, 131.1, 130.6, 130.5, 130.3, 129.1, 127.1, 127.0, 126.2, 126.0, 125.7, 125.6, 124.8, 124.5, 124.5, 123.9, 123.7, 121.4, 36.4, 33.4, 32.4, 30.8, 30.4, 30.3, 30.3, 30.2, 30.1, 29.9, 23.2, 21.5, 21.0, 14.4; FD-MS (8 kV): *m/z* 1045.9; HRMS (MALDI-TOF): *m/z* Calcd for $C_{80}H_{84}$: 1044.6573 $[M]^+$, found:1044.6477.

3. DFT Calculations

DFT calculations were performed using the Gaussian 09 software package.[1] The geometry and energies were calculated at the B3LYP/6-311G(d,p) level. Time-dependent DFT (TDDFT) calculations were performed at the same level of theory. Methyl groups were used to replace the long dodecyl chains for computational simplicity.

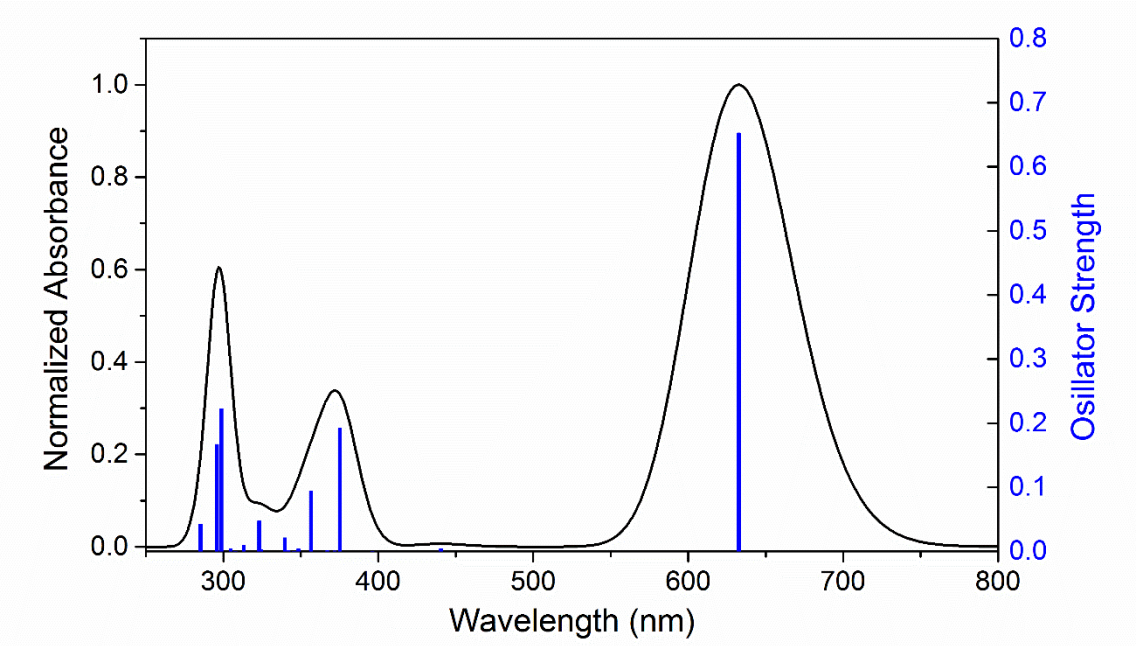

Figure S1. Simulated absorption spectrum of DBO **1** and the oscillator strengths (blue bars) by TDDFT calculations at the B3LYP/6-311G(d,p) level.

Table S1. Major electronic transitions of DBO **1** calculated by TDDFT method.

excited state	energy (eV)	wavelength (nm)	oscillator strength	description
1	1.96	633	0.6525	HOMO→LUMO (0.70333)
2	3.30	375	0.1921	HOMO–2→LUMO (0.46008) HOMO–1→LUMO+1 (0.19231) HOMO→LUMO+2 (0.37460) HOMO→LUMO+5 (0.29962)
3	3.48	356	0.0939	HOMO–9→LUMO (0.15490) HOMO–2→LUMO (–0.19955) HOMO→LUMO+2 (–0.16608) HOMO→LUMO+5 (0.60927) HOMO→LUMO+6 (0.13137)
4	3.65	340	0.0208	HOMO–10→LUMO (0.17297) HOMO–9→LUMO (–0.16125) HOMO→LUMO+6 (0.62283) HOMO→LUMO+8 (0.16131)
5	4.19	296	0.1668	HOMO–10→LUMO (–0.12649) HOMO–3→LUMO+1 (0.43824) HOMO–1→LUMO+1 (–0.34967) HOMO–1→LUMO+3 (0.31913) HOMO–1→LUMO+4 (–0.13474)

Table S2. Cartesian coordinates of the DFT-optimized **1**.

Tag	Symbol	X	Y	Z
1	C	-4.2849776	-3.878662	-0.3125137
2	C	-2.9033849	-4.0084556	-0.2339019
3	C	-2.0848278	-2.8954912	-0.1089299
4	C	-2.6936236	-1.6000378	-0.0825411
5	C	-4.1384394	-1.4626524	-0.122407
6	C	-4.9342381	-2.6582696	-0.2560758

7	C	-1.8522722	-0.4469504	-0.0284391
8	C	-2.4315207	0.8376813	0.0200664
9	C	-3.8600291	0.9764682	0.0490043
10	C	-4.6954394	-0.1457472	-0.0261328
11	C	-1.6001654	1.9984213	0.0479767
12	C	-2.1882838	3.2900516	0.1258445
13	C	-3.6126709	3.4029481	0.189184
14	C	-4.4075029	2.3074597	0.1536298
15	C	-0.6335217	-3.0313979	-0.011688
16	C	0.1814169	-1.8720788	-0.0030873
17	C	-0.4125554	-0.5717634	-0.0258575
18	C	0.4125636	0.5717923	-0.025836
19	C	-0.1814101	1.8721061	-0.0030087
20	C	0.6335281	3.031426	-0.0115714
21	C	0.0132615	4.2892975	0.0798176
22	C	-1.358284	4.4171241	0.1498933
23	C	-0.0132571	-4.2892722	0.0796697
24	C	1.3582888	-4.4171025	0.1497299
25	C	2.18829	-3.2900305	0.125702
26	C	1.6001718	-1.9983967	0.0478847
27	C	2.4315272	-0.8376555	0.0200129
28	C	1.8522812	0.4469797	-0.0284321
29	C	2.6936346	1.6000699	-0.0824828
30	C	2.0848354	2.8955245	-0.1088069
31	C	3.6126781	-3.4029311	0.1890145

32	C	4.4075102	-2.3074416	0.1534897
33	C	3.8600349	-0.9764456	0.0489316
34	C	4.6954494	0.1457697	-0.0261544
35	C	4.1384543	1.4626873	-0.1223545
36	C	4.9342491	2.6583204	-0.2559564
37	C	4.2849825	3.8787131	-0.3123215
38	C	2.9033902	4.0084983	-0.2337058
39	C	-6.173161	0.1258684	0.0238216
40	C	-6.4432334	-2.7205367	-0.3664372
41	C	6.1731658	-0.1258779	0.0237803
42	C	6.4432427	2.7206217	-0.3663245
43	C	6.8752516	-0.4554522	-1.1512573
44	C	8.2362486	-0.7559957	-1.0695056
45	C	8.922118	-0.7506826	0.1458603
46	C	8.2020847	-0.4458177	1.3008265
47	C	6.839761	-0.1382551	1.2629954
48	C	-6.8752607	0.4554931	-1.1512017
49	C	-8.236259	0.7559931	-1.0694333
50	C	-8.922132	0.7505844	0.145938
51	C	-8.2020971	0.4456542	1.3008772
52	C	-6.8397583	0.1381301	1.2630286
53	C	-10.401619	1.0465204	0.2041211
54	C	10.4016028	-1.0466248	0.2040553
55	H	-4.881453	-4.7774028	-0.4248885
56	H	-2.4812906	-5.001824	-0.2904543

57	H	-4.0490219	4.3935348	0.2650351
58	H	-5.4809781	2.4231607	0.20177
59	H	0.6123406	5.1886414	0.110089
60	H	-1.8070904	5.4019416	0.2250289
61	H	-0.6123388	-5.1886144	0.1099303
62	H	1.8070948	-5.4019221	0.2248377
63	H	4.0490296	-4.393521	0.2648191
64	H	5.4809876	-2.4231433	0.2016047
65	H	4.8814549	4.7774635	-0.4246396
66	H	2.4812951	5.0018704	-0.2901945
67	H	-6.8294313	-2.1441224	-1.2072568
68	H	-6.7427924	-3.7600551	-0.5128143
69	H	-6.9521527	-2.3531478	0.5253575
70	H	6.8294421	2.144293	-1.2072026
71	H	6.7427796	3.7601598	-0.5126106
72	H	6.9521799	2.3531638	0.5254308
73	C	6.1801614	-0.4881554	-2.4927408
74	H	8.7733124	-1.0041891	-1.9805412
75	H	8.7111221	-0.4513825	2.2603256
76	C	6.1060482	0.1740709	2.5467256
77	C	-6.1801691	0.4882945	-2.4926821
78	H	-8.7733286	1.0042301	-1.9804545
79	H	-8.7111383	0.4511332	2.2603738
80	C	-6.1060479	-0.1742682	2.5467426
81	H	-10.6924111	1.7768926	-0.5548705

82	H	-10.991139	0.1401655	0.0268529
83	H	-10.6917257	1.4390197	1.181392
84	H	10.6926581	-1.7758867	-0.5558958
85	H	10.9911231	-0.1399777	0.0282839
86	H	10.6914469	-1.440507	1.180852
87	H	-6.7798312	-0.1139768	3.4033712
88	H	-5.2806526	0.5233772	2.7143594
89	H	-5.6703403	-1.1777032	2.5292686
90	H	-6.8945874	0.6810865	-3.2952086
91	H	-5.6725413	-0.4561355	-2.7090541
92	H	-5.4157462	1.2701164	-2.5267243
93	H	6.7798147	0.1136672	3.4033597
94	H	5.2806096	-0.5235414	2.7142677
95	H	5.6703981	1.1775333	2.5293311
96	H	6.8945802	-0.6808872	-3.2952815
97	H	5.6725311	0.4562899	-2.7090418
98	H	5.4157397	-1.2699771	-2.5268406

Reference:

1. Gaussian 09, Revision D.01, Frisch, M. J.; Trucks, G. W.; Schlegel, H. B.; Scuseria, G. E.; Robb, M. A.; Cheeseman, J. R.; Scalmani, G.; Barone, V.; Mennucci, B.; Petersson, G. A.; Nakatsuji, H.; Caricato, M.; Li, X.; Hratchian, H. P.; Izmaylov, A. F.; Bloino, J.; Zheng, G.; Sonnenberg, J. L.; Hada, M.; Ehara, M.; Toyota, K.; Fukuda, R.; Hasegawa, J.; Ishida, M.; Nakajima, T.; Honda, Y.; Kitao, O.; Nakai, H.; Vreven, T.; Montgomery, Jr., J. A.; Peralta, J. E.; Ogliaro, F.; Bearpark, M.; Heyd, J. J.; Brothers, E.; Kudin, K. N.; Staroverov, V. N.; Kobayashi, R.; Normand, J.; Raghavachari,

K.; Rendell, A.; Burant, J. C.; Iyengar, S. S.; Tomasi, J.; Cossi, M.;Rega, N.; Millam, N. J.; Klene, M.; Knox, J. E.; Cross, J. B.; Bakken, V.; Adamo, C.; Jaramillo, J.; Gomperts, R.; Stratmann, R. E.; Yazyev, O.; Austin, A. J.; Cammi, R.; Pomelli, C.; Ochterski, J. W.; Martin, R. L.; Morokuma, K.; Zakrzewski, V. G.; Voth, G. A.; Salvador, P.; Dannenberg, J. J.; Dapprich, S.; Daniels, A. D.; Farkas, Ö.; Foresman, J. B.; Ortiz, J. V.; Cioslowski, J.; Fox, D. J. Gaussian, Inc., Wallingford CT, 2013.

4. Cyclic voltammetry

The cyclic voltammetry (CV) of DBO **1** was measured in dichloromethane solution with *n*-Bu_4NPF_6 (0.1 M) at a scan rate of 50 mV/s at room temperature. The HOMO and LUMO energy levels were calculated according to the following equations: HOMO = $-(4.8+E_{ox}^{onset})$ and LUMO = $-(4.8+E_{red}^{onset})$, where E_{ox}^{onset} and E_{red}^{onset} referred to the onset potentials of the first oxidative and reductive redox waves, respectively.

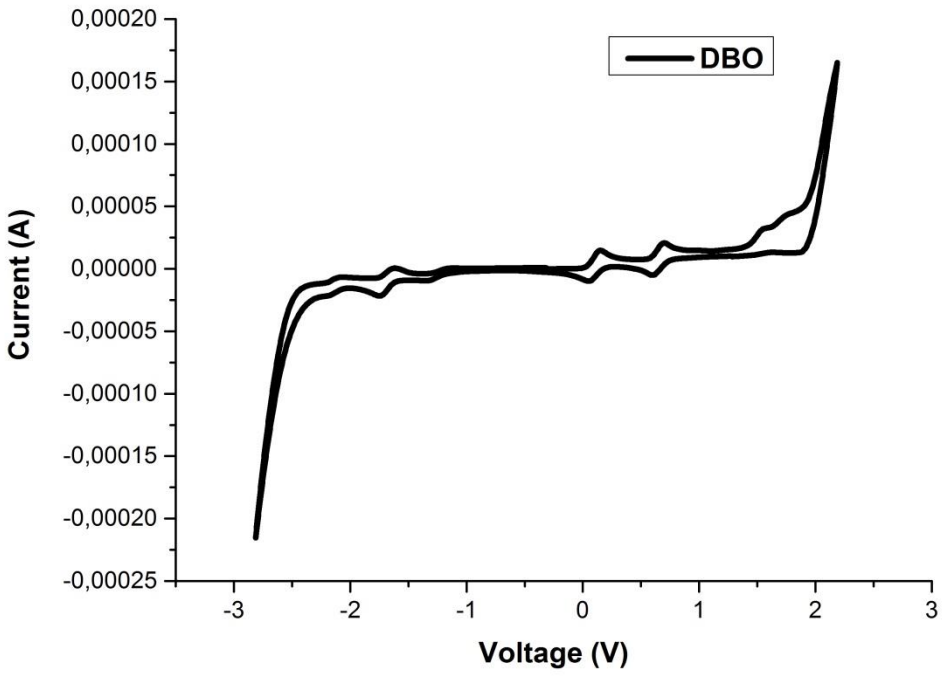

Figure S2. Cyclic voltammogram of DBO **1** vs Fc/Fc^+ (0.1 M nBu_4NPF_6 in dichloromethane solution), scan rate 50 mVs^{-1}.

5. Supplementary transient absorption data

The transient spectra (a) and time-decay dynamics till 1 ns (b) of DBO **1** in toluene are presented in Figure S3. We can see that all the signals are relatively long-living (Supplementary Fig. S3b), with time-constants $\tau_{430\ nm}$ = 432 ± 35 ps, $\tau_{570\ nm}$ = 280 ± 5 ps, $\tau_{650\ nm}$ = 302 ± 5 ps and $\tau_{695\ nm}$ = 292 ± 7 ps. We can also observe a sharp rise of all the transient signals (c) and a linear dependence on pump fluence (d), which suggest that the photoexcitation mechanism is direct and does not involve any non-linear process.

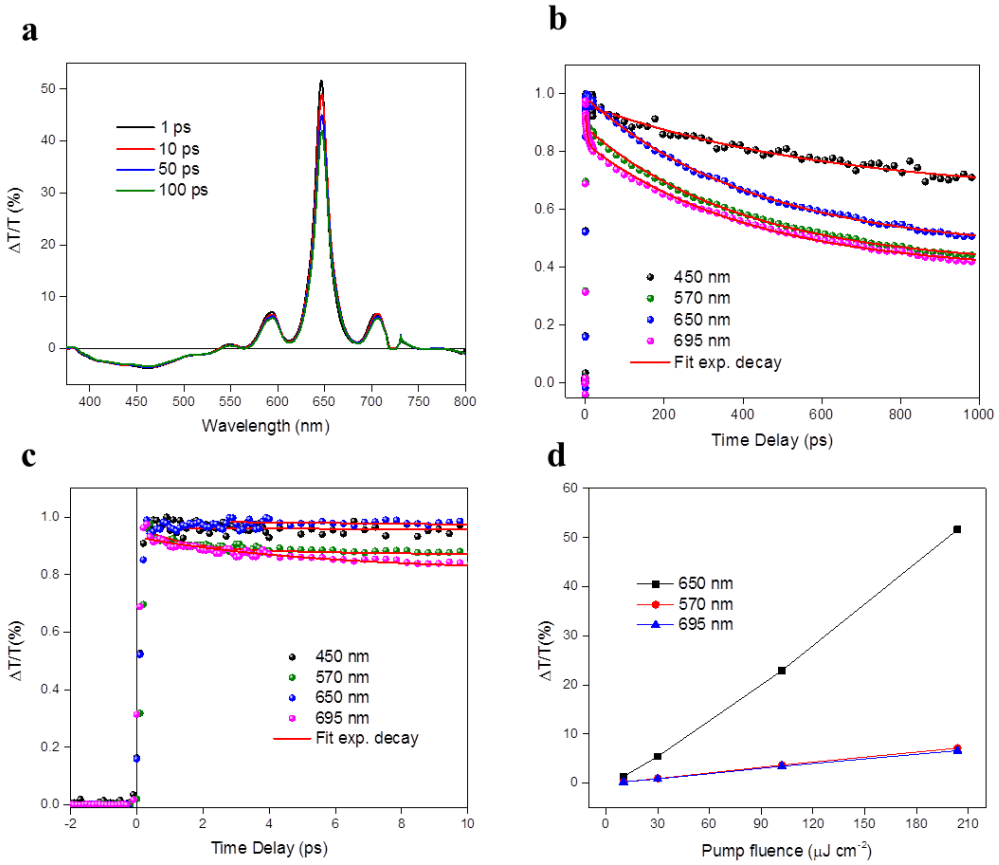

Figure S3. a) Transient spectra of DBO **1** in solution as a function of pump-probe delay time (0.05 mg/mL in toluene). b) Dynamics at 450 nm, 570nm, 630 nm and 695 nm probe wavelengths. c) Rise time of the transient signals. d) Signal intensities vs. Pump fluence.

In figure S4 we show the transient spectra of the soluble hexa-perihexabenzocoronene (HBC) derivative, which features an armchair edge structure. The spectra were taken at three concentrations, 0.1 mg/mL, 0.05 mg/mL and 0.01 mg/mL in toluene. We can observe a strong PA signal that incorporates all the transient features in the probed spectral range (from 430 nm to 650 nm), and hinders the appearance of any SE signal.

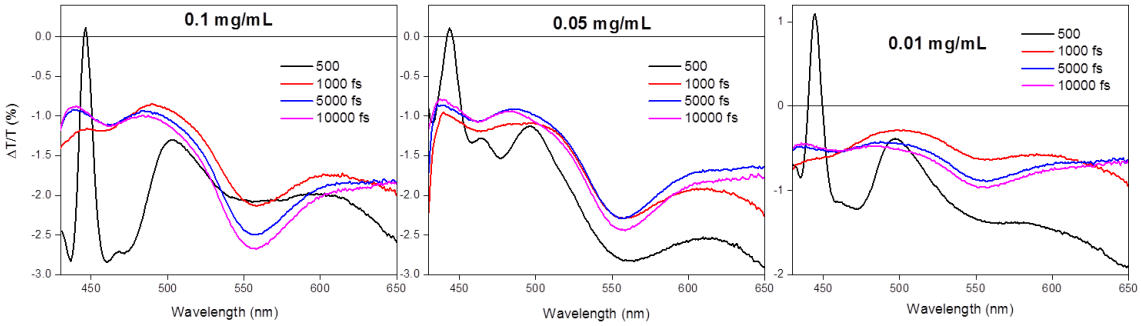

Figure S4. Transient spectra for of the soluble hexa-perihexabenzocoronene (HBC) derivative with armchair edge structure. The spectra were taken in toluene solution at three different concentrations (0.1 mg/mL, 0.05 mg/mL and 0.01 mg/mL).

In figure S5, we report the transient spectra (a) and dynamics (b) of DBO **1** in film. We can note a clear broadening of all the transient features and a step decrease of all the transient signal lifetimes. The calculated time-constants are: τ_{430} nm = 15.2 ± 0.7 ps, τ_{570} nm = 12 ± 6 ps and τ_{650} nm = 7.9 ± 0.3 ps. The SE signal at 695 nm is completely overwhelmed in ≈ 200 fs by a long-living PA signal.

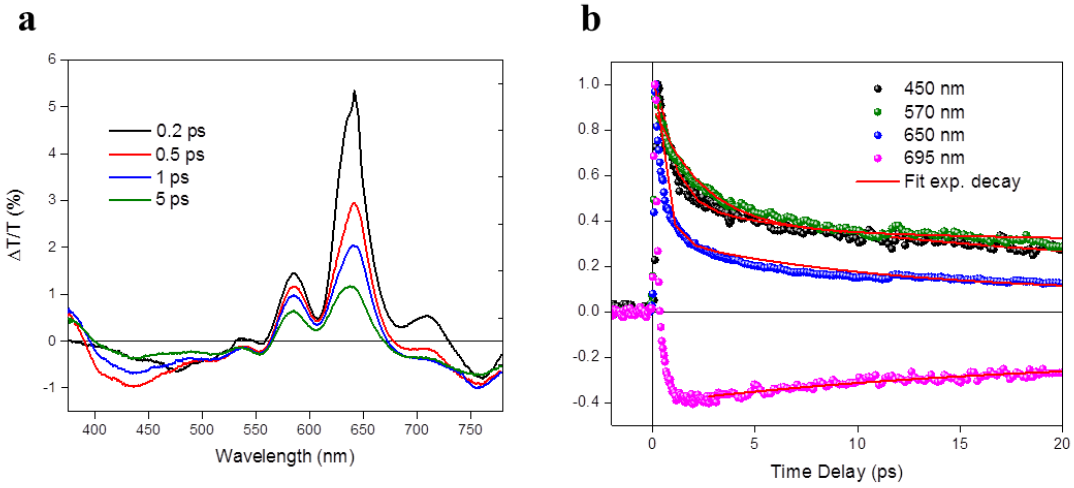

Figure S5. a) Transient spectra of DBO **1** in film as a function of pump-probe delay time. b) Dynamics at 450 nm, 570nm, 630 nm and 695 nm probe wavelengths.

By blending the DBO **1** with PS we note a general increase of life-times and a recover of the SE signal from the large PA. Interestingly, the DBO **1** : PS 1 $_w$% blend shows similar transient features with the ones observed in solution, with a relatively narrow PB peak and a suppressed PA signal.

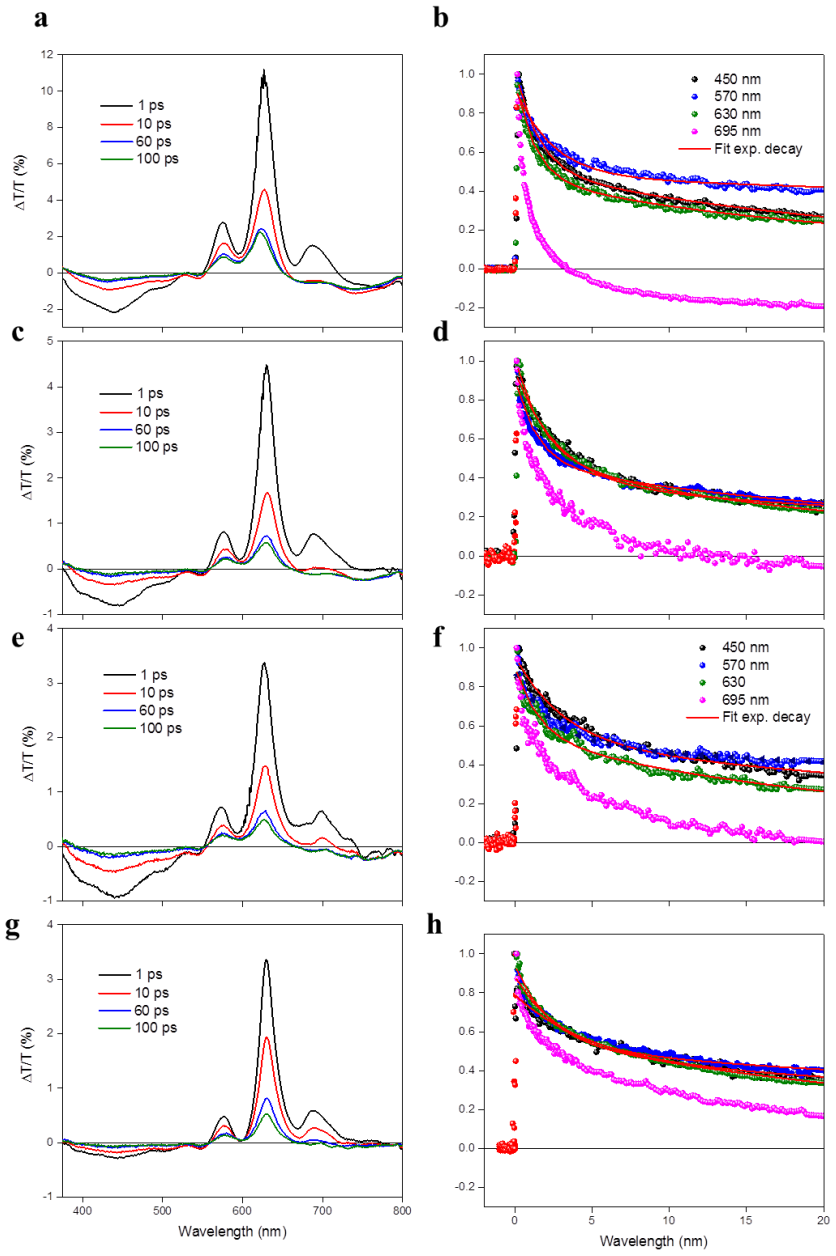

Figure S6. Transient spectra for a) DBO 1:PS 10 $_w$%, (c) 5 $_w$%, (e) 3 $_w$% and (g) 1 $_w$% blends. Normalised time-decay dynamics for b) DBO 1:PS 10 $_w$%, d) 5 $_w$%, f) 3 $_w$% and h) 1 $_w$% blends.

6. Supplementary PL measurements

We also observed line narrowing for the DBO **1**:PS 3 $_{w}$% composite film, with a threshold lying at ≈ 150 μW cm^{-2} (a-b). For 5 $_{w}$% and 10 $_{w}$% blends, we were able to observe a recovery of the PL, which was completely suppressed in pure DBO **1** films (c-d).

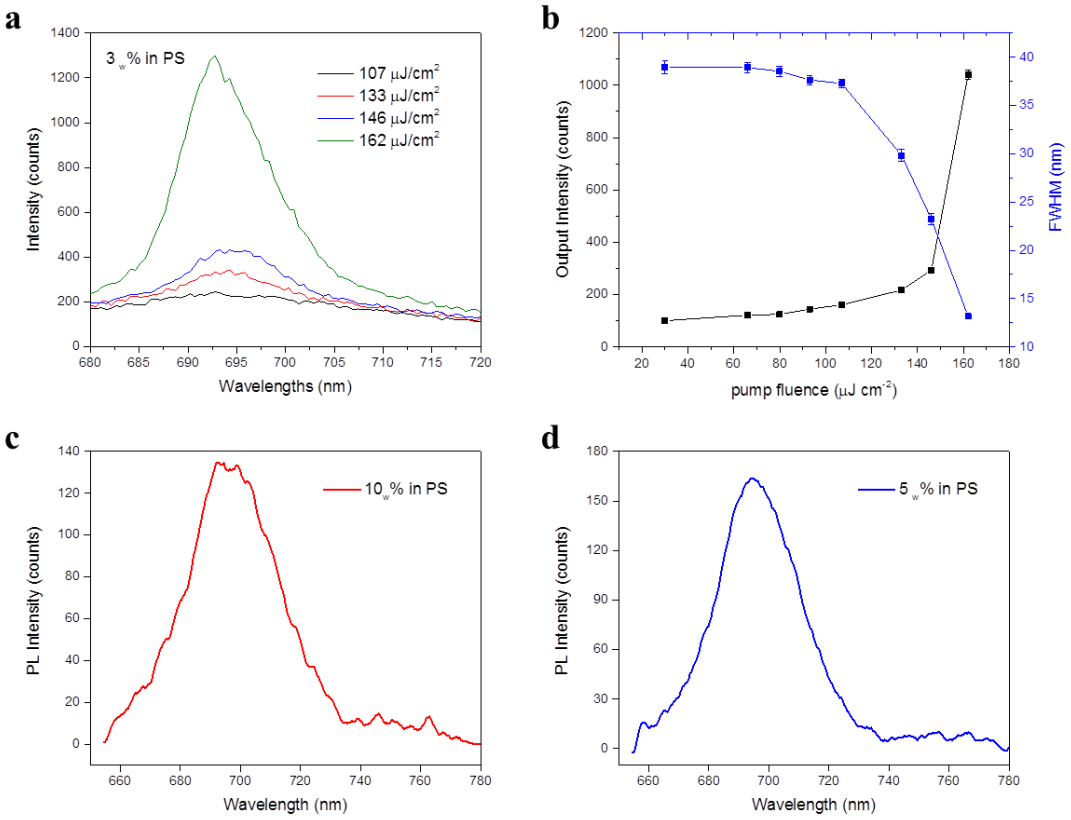

Figure S7. a) PL for different pump power from the DBO 1:PS 3 $_{w}$% composite film and b) input-output characteristics of ASE action for the 3 w% blend in PS. c) PL from the DBO 1:PS 10 $_{w}$% and d) PL from the DBO 1:PS 5 $_{w}$%.

7. NMR and HRMS spectra

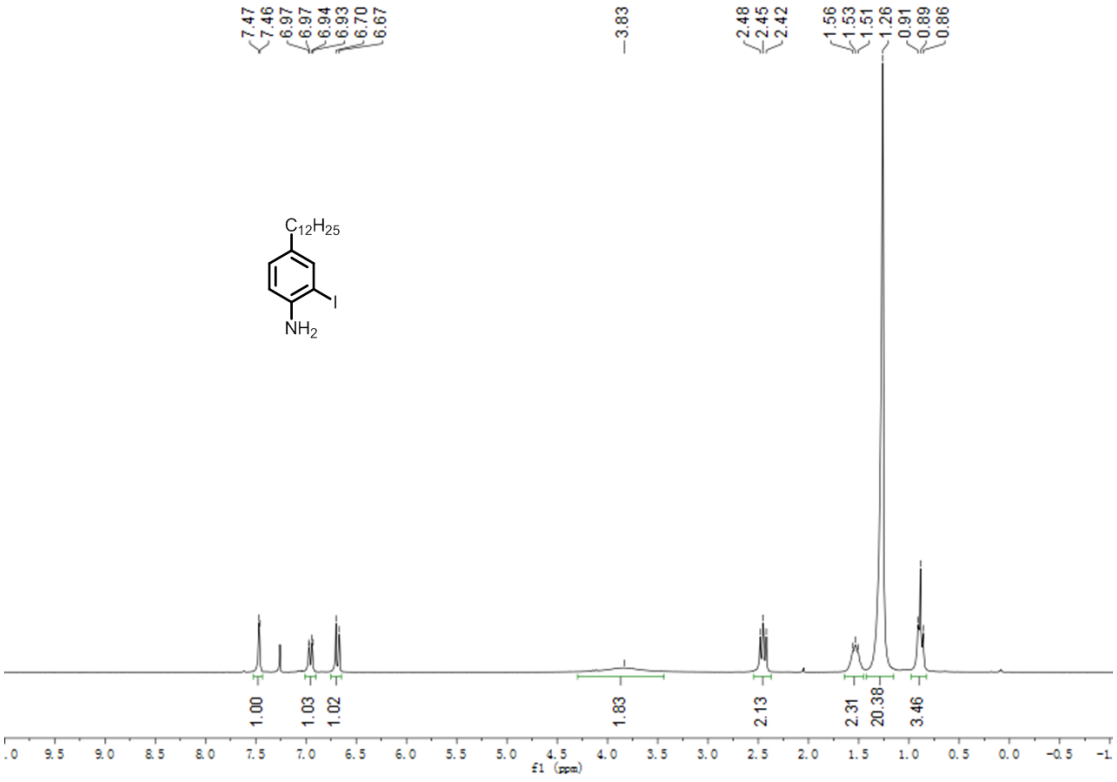

Figure S8. ^{1}H NMR spectrum of compound **S2** in CD_2Cl_2 (250 MHz, 298 K).

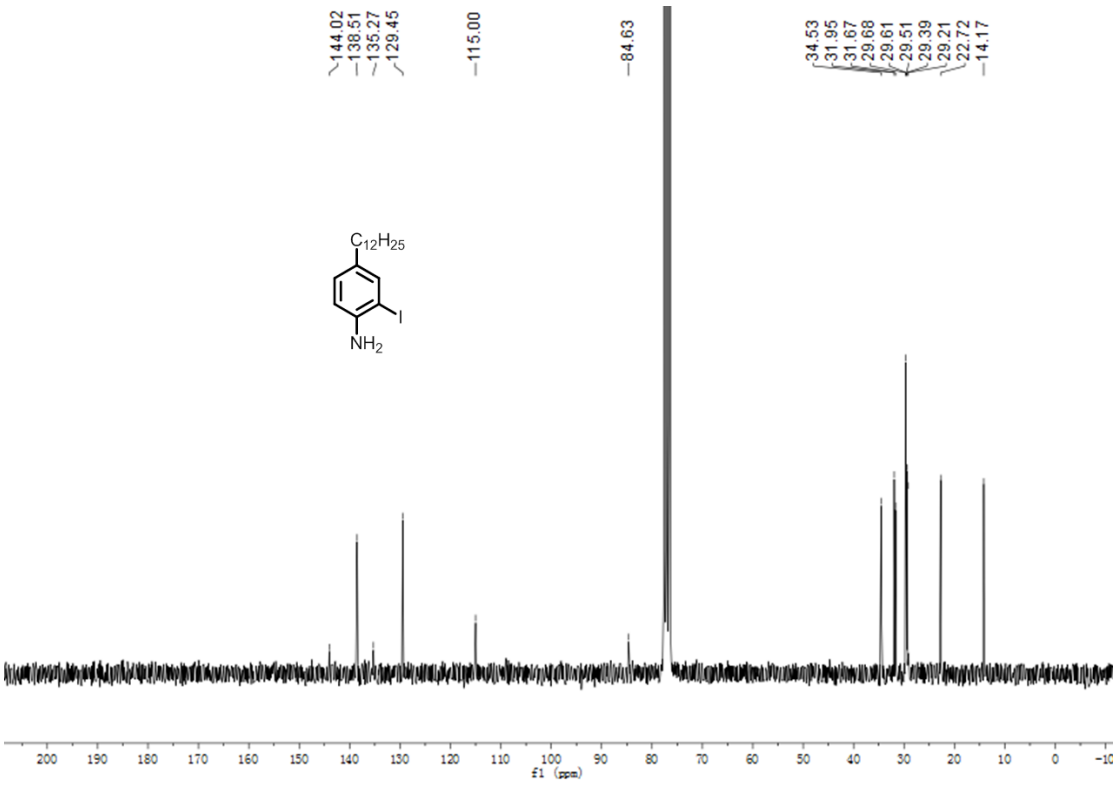

Figure S9 . ^{13}C NMR spectrum of **S2** in CD_2Cl_2 (62.5 MHz, 298 K).

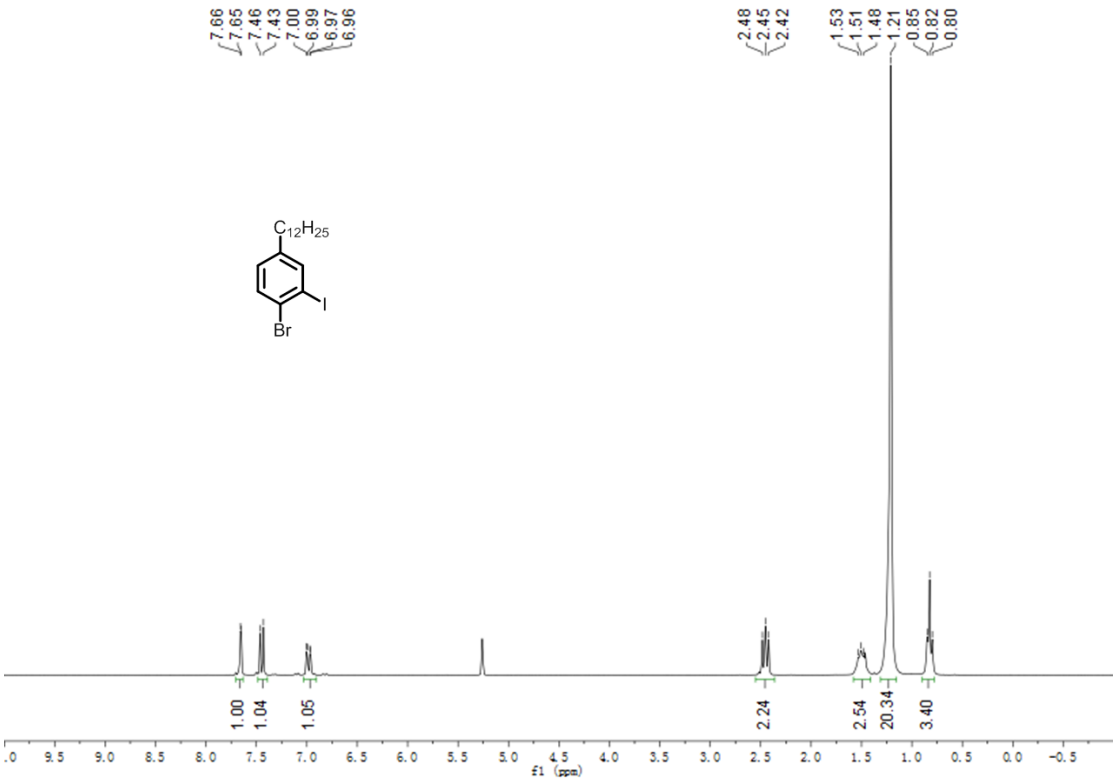

Figure S10. ^{1}H NMR spectrum of compound **S3** in CD_2Cl_2 (250 MHz, 298 K).

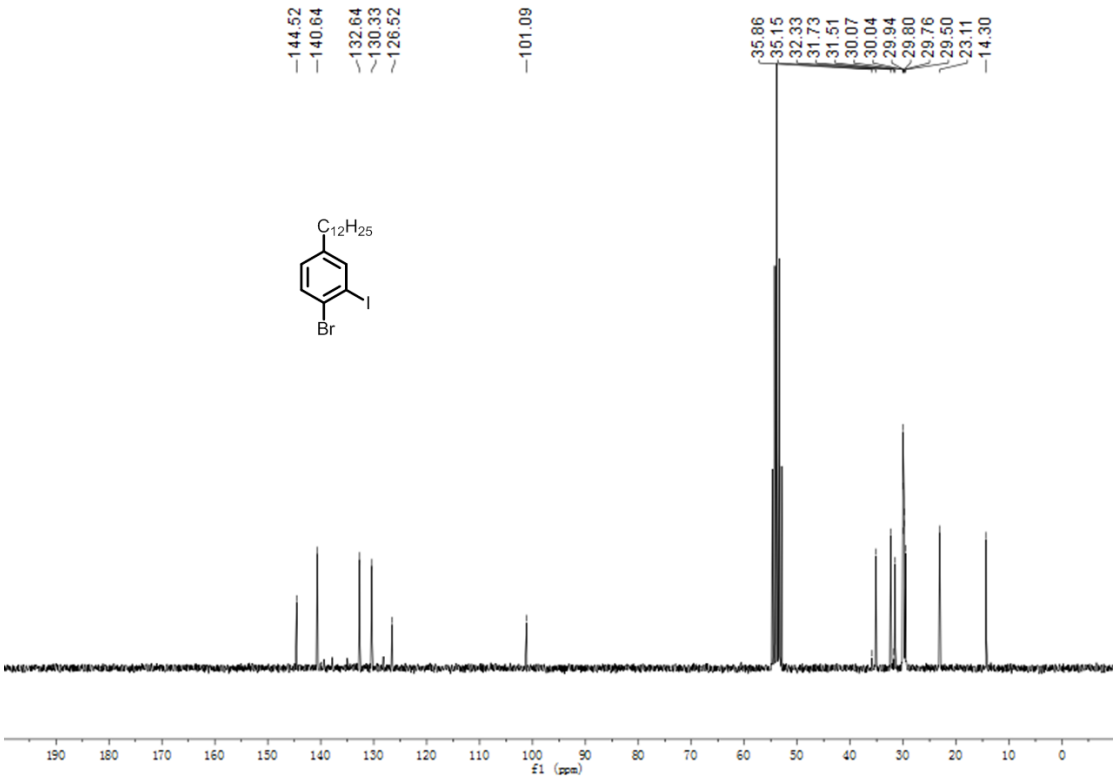

Figure S1. ^{13}C NMR spectrum of compound **S3** in CD_2Cl_2 (62.5 MHz, 298 K).

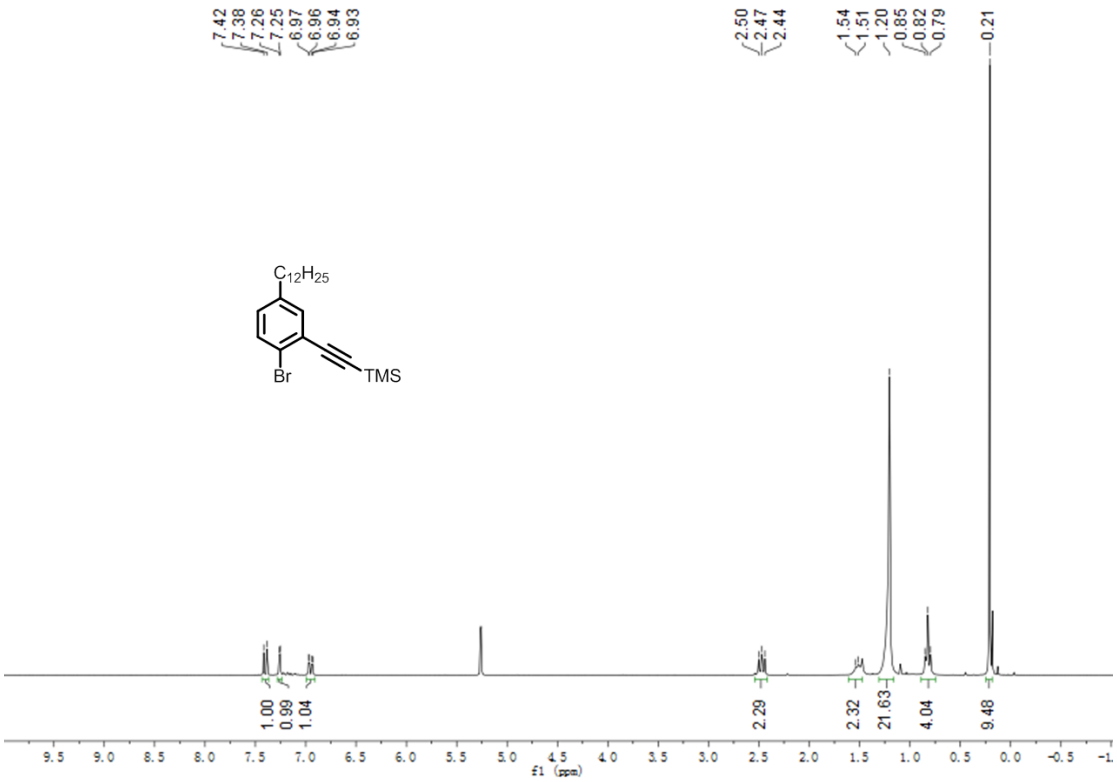

Figure S12. ^{1}H NMR spectrum of compound **S4** in CD_2Cl_2 (250 MHz, 298 K).

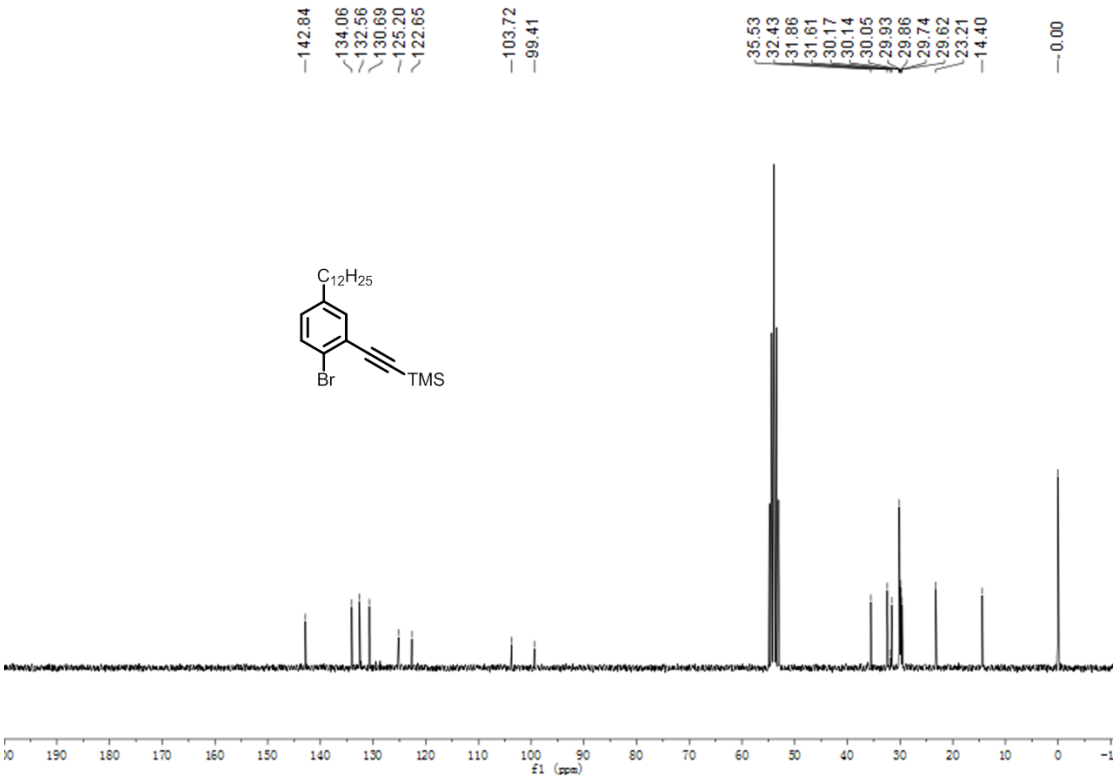

Figure S13. ^{13}C NMR spectrum of compound **S4** in CD_2Cl_2 (62.5 MHz, 298 K).

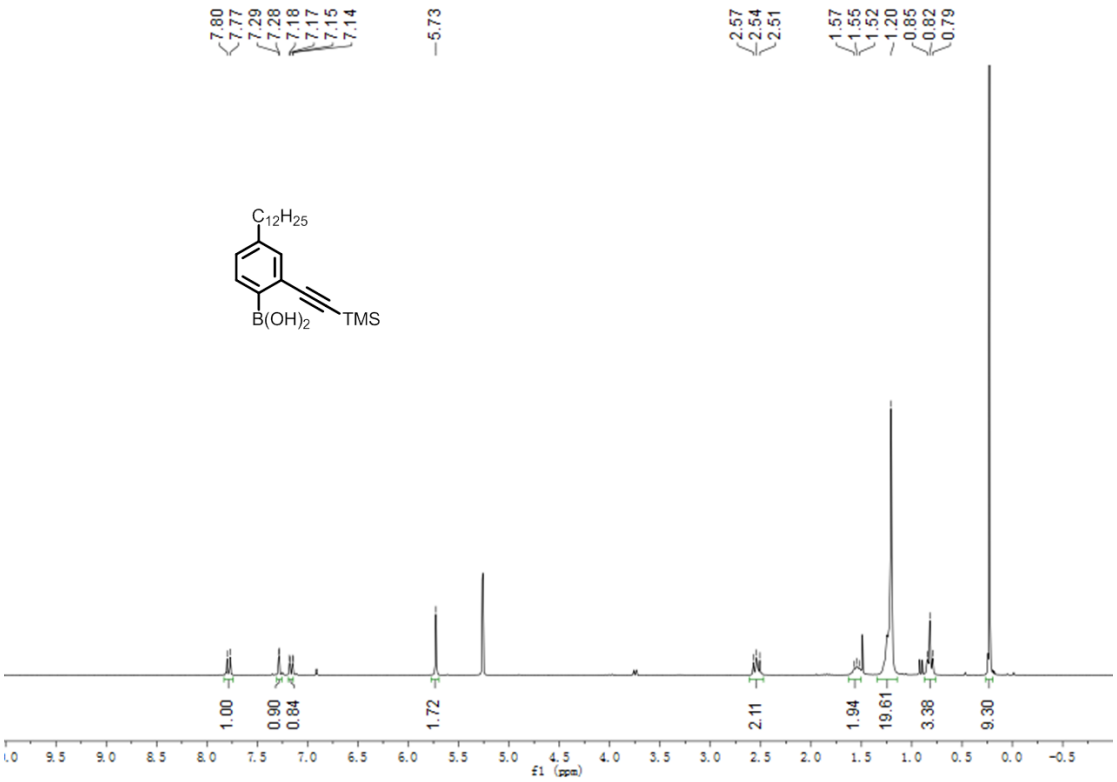

Figure S14. ^{1}H NMR spectrum of compound **2** in CD_2Cl_2 (250 MHz, 298 K).

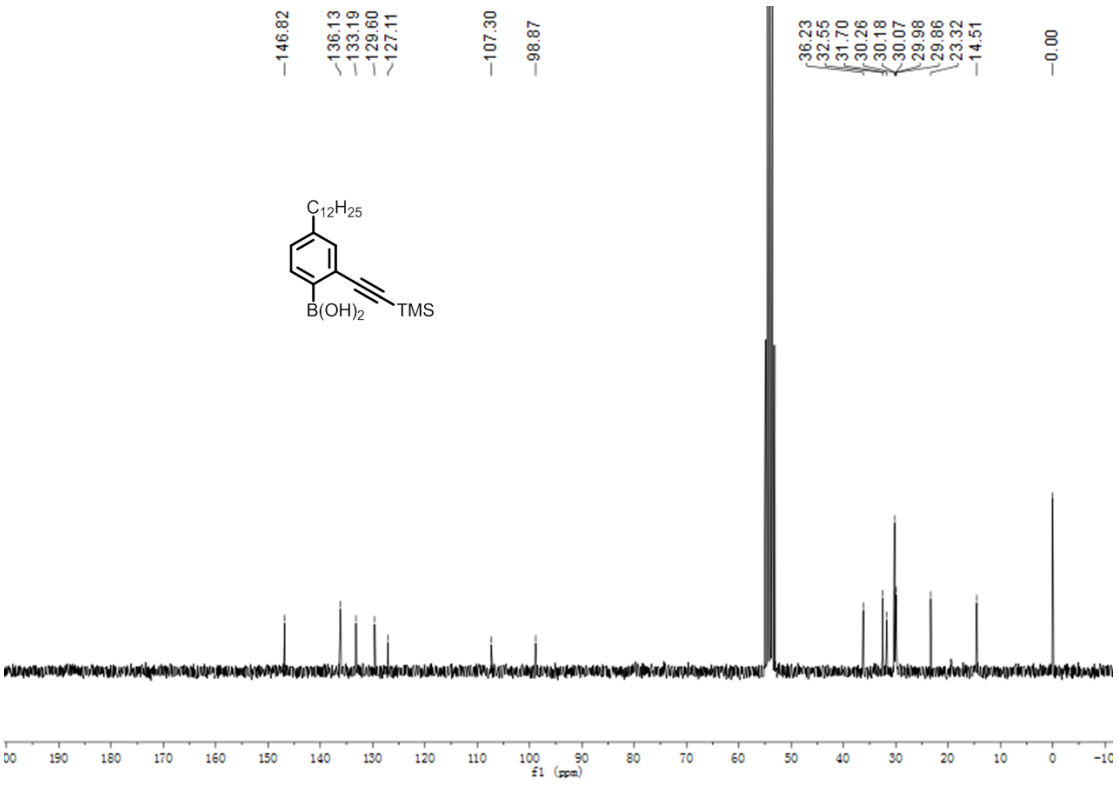

Figure S15. ^{13}C NMR spectrum of compound **2** in CD_2Cl_2 (62.5 MHz,

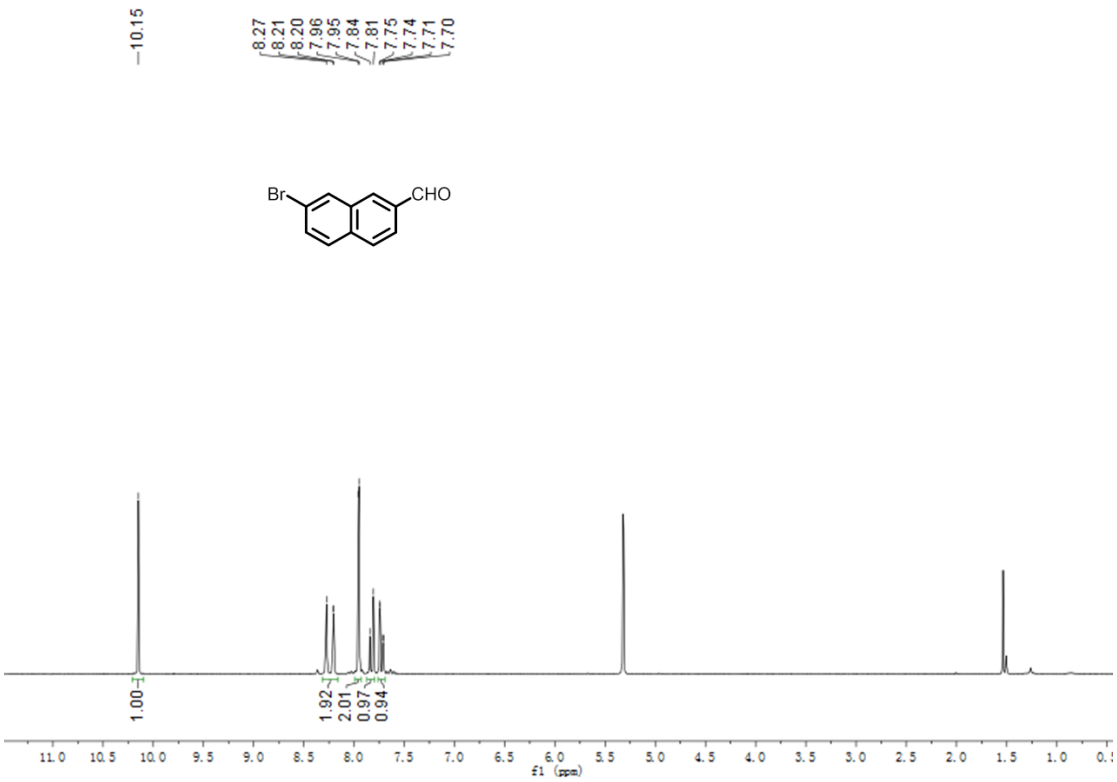

Figure S16. ^{1}H NMR spectrum of compound **3** in CD_2Cl_2 (250 MHz, 298 K).

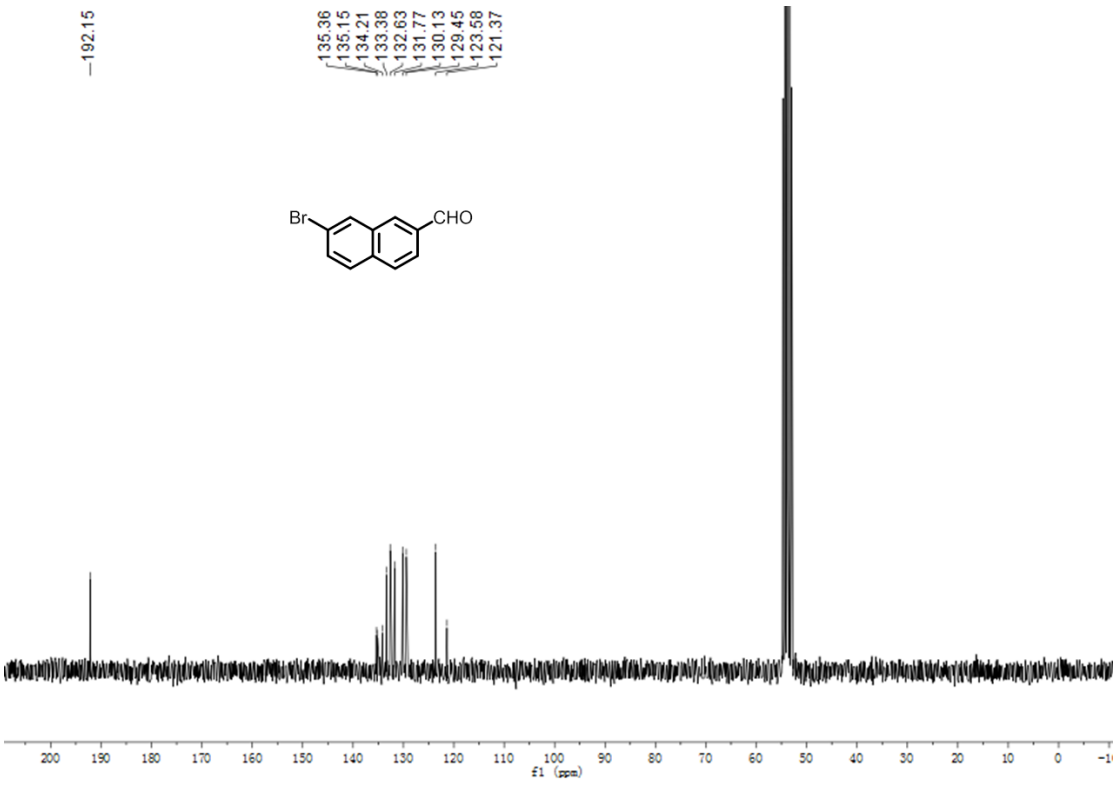

Figure S17. ^{13}C NMR spectrum of compound **3** in CD_2Cl_2 (62.5 MHz, 298 K).

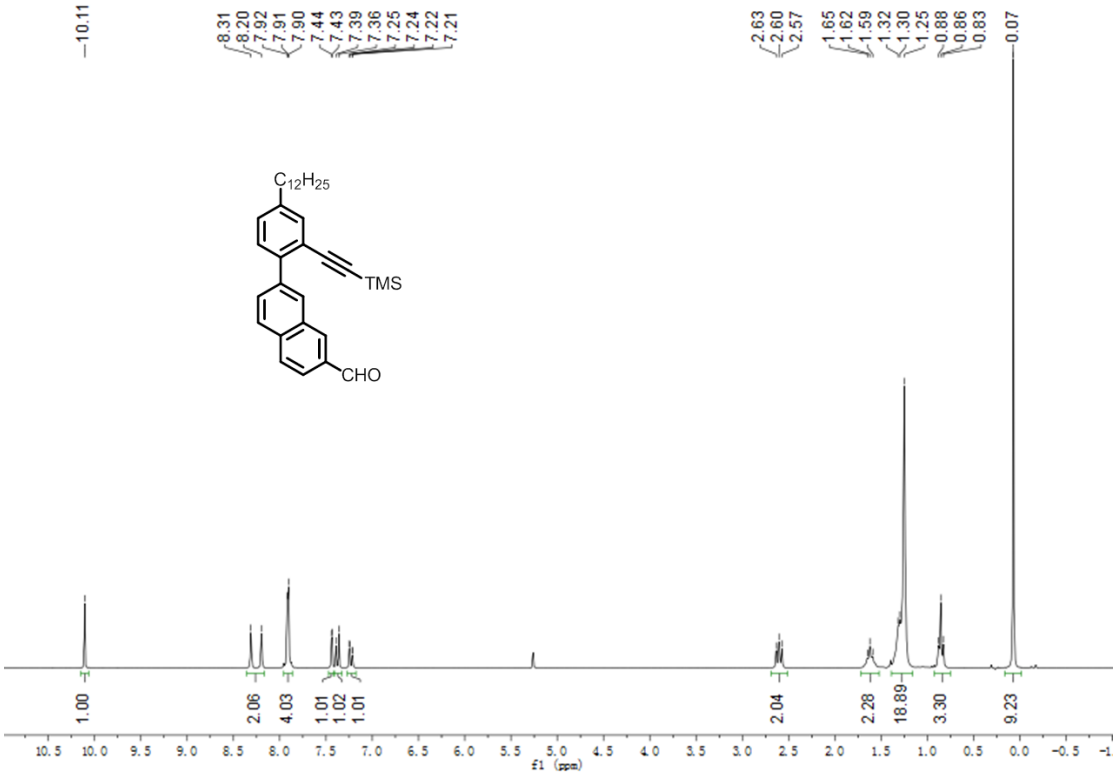

Figure S18. ^{1}H NMR spectrum of compound **4** in CD_2Cl_2 (250 MHz, 298 K).

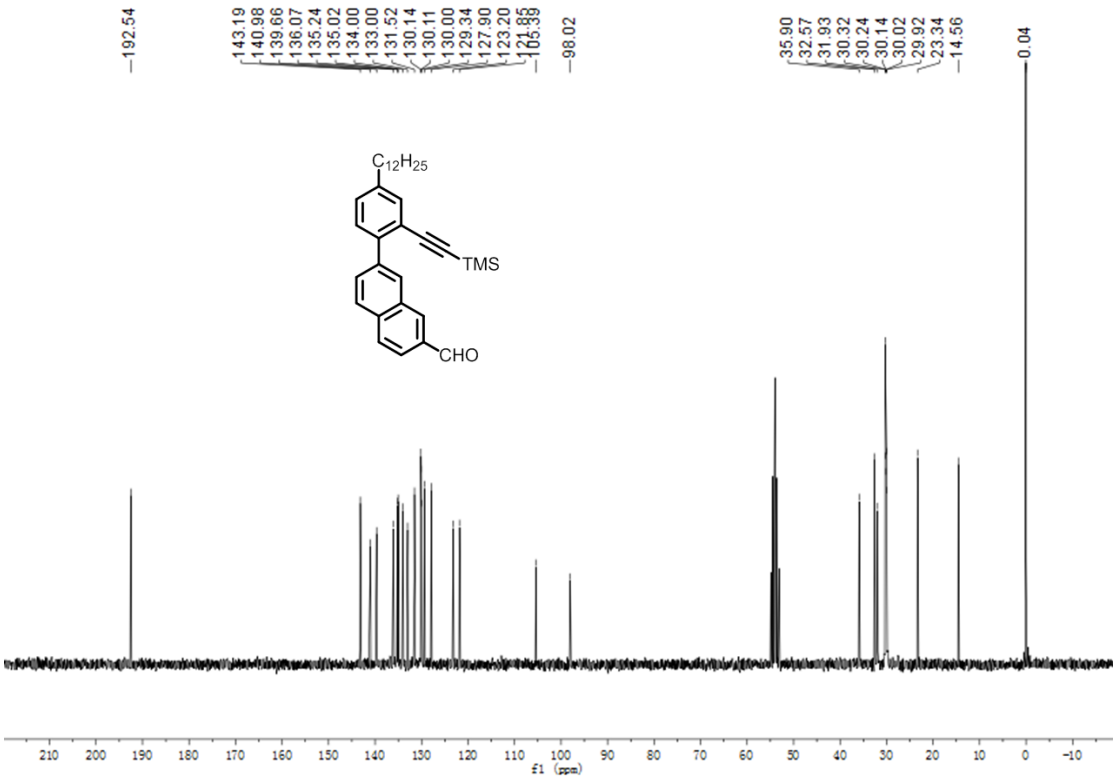

Figure S19. ^{13}C NMR spectrum of compound **4** in CD_2Cl_2 (62.5 MHz, 298 K).

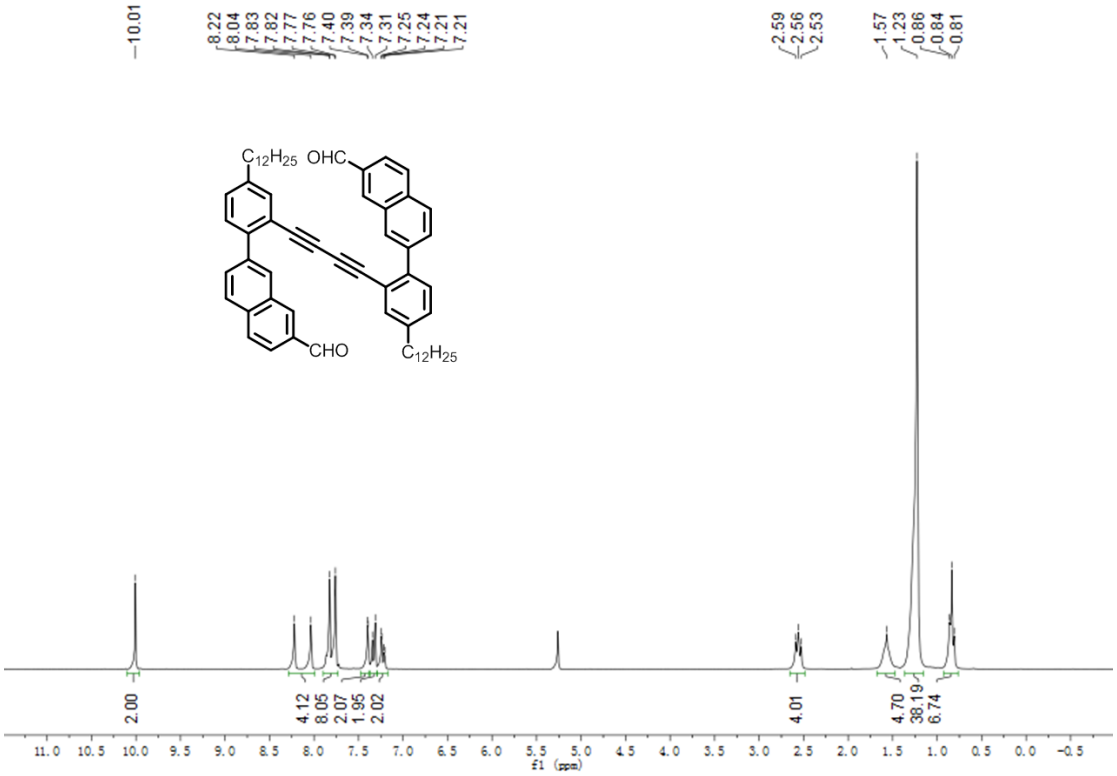

Figure S20. ^{1}H NMR spectrum of compound **5** in CD_2Cl_2 (250 MHz, 298 K).

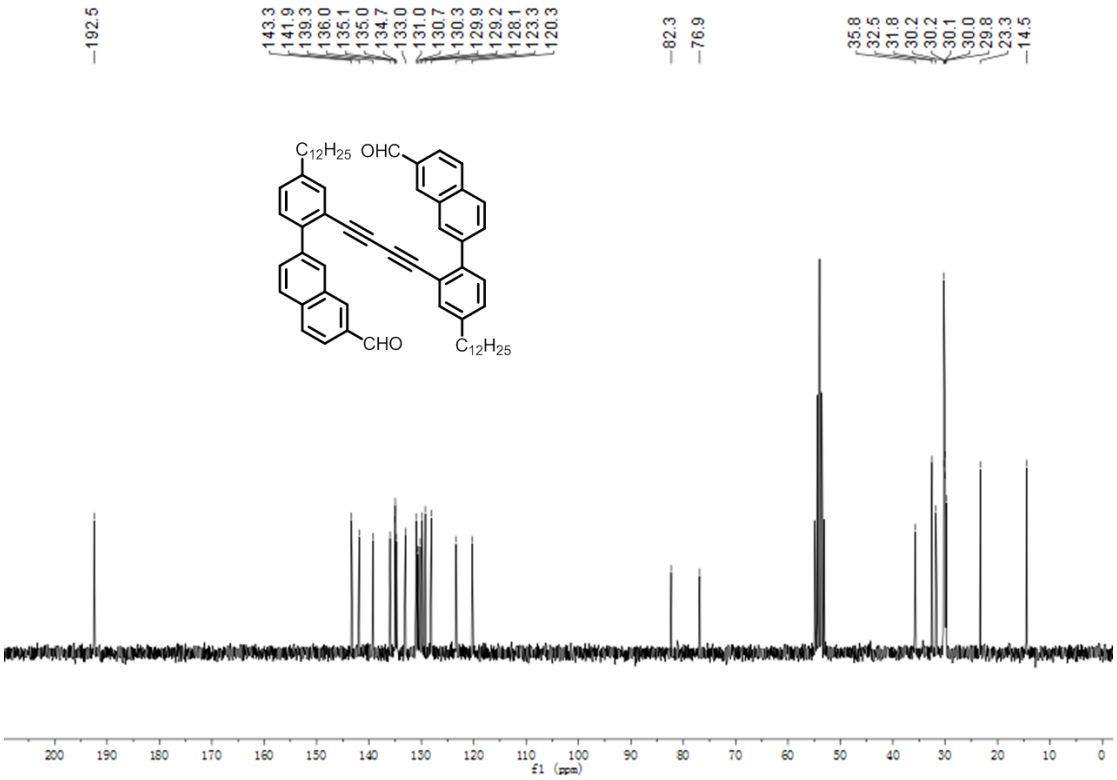

Figure S21. ^{13}C NMR spectrum of compound **5** in CD_2Cl_2 (62.5 MHz, 298 K).

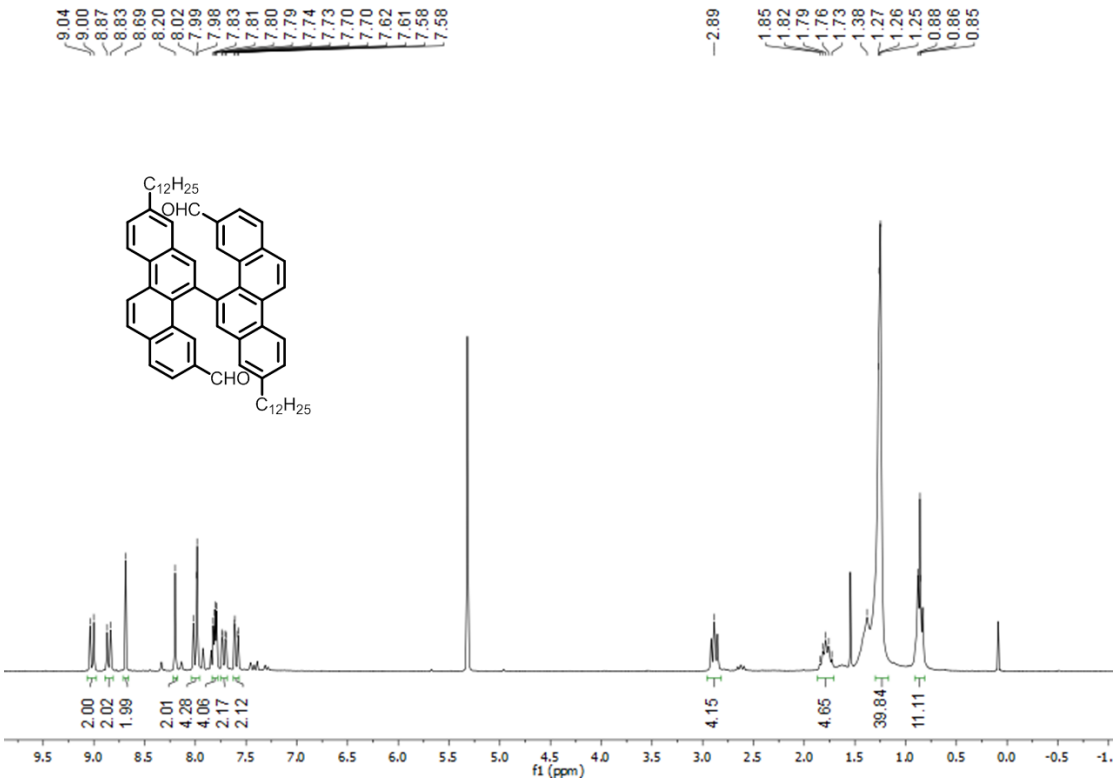

Figure S22. ^{1}H NMR spectrum of compound **6** in CD_2Cl_2 (250 MHz, 298 K).

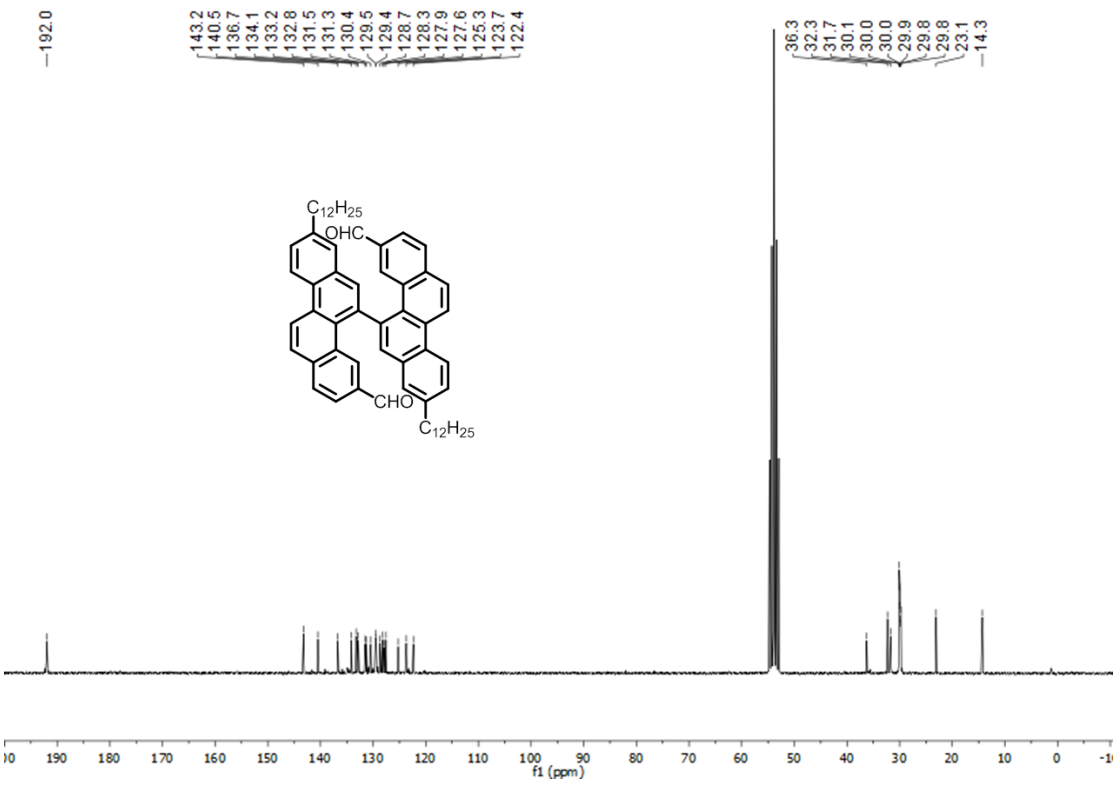

Figure S23. ^{13}C NMR spectrum of compound **6** in CD_2Cl_2 (62.5 MHz, 298 K).

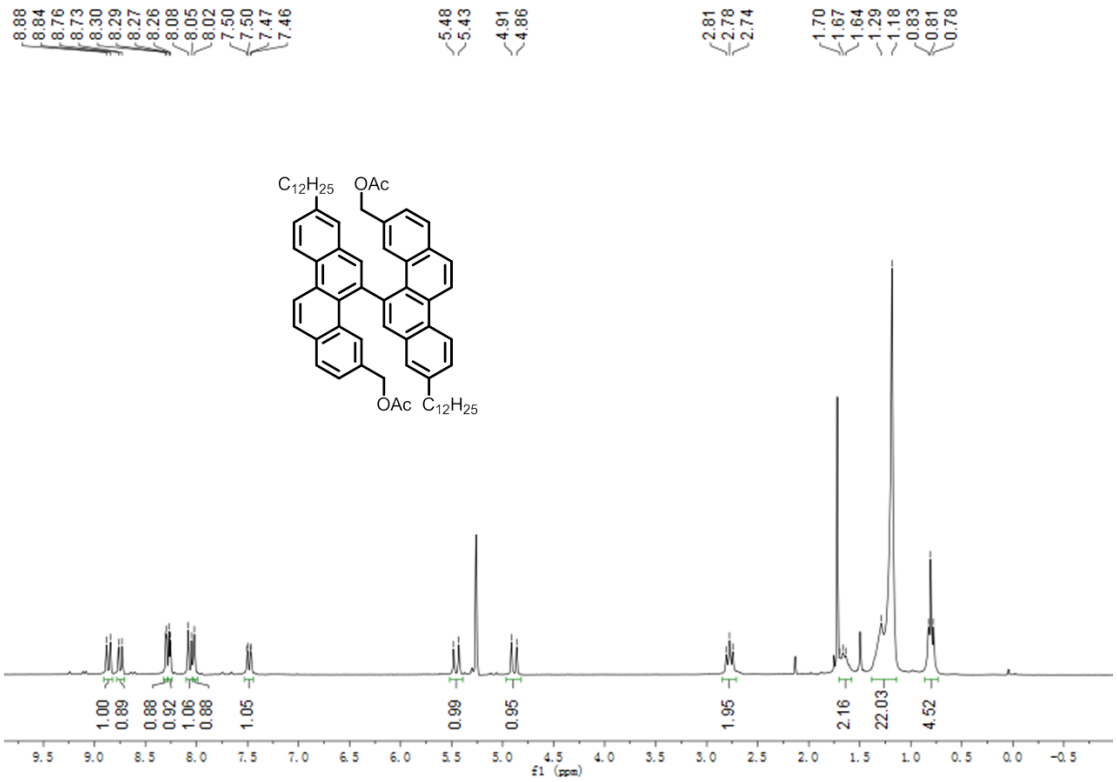

Figure S24. ^{1}H NMR spectrum of compound **7** in CD_2Cl_2 (250 MHz, 298 K).

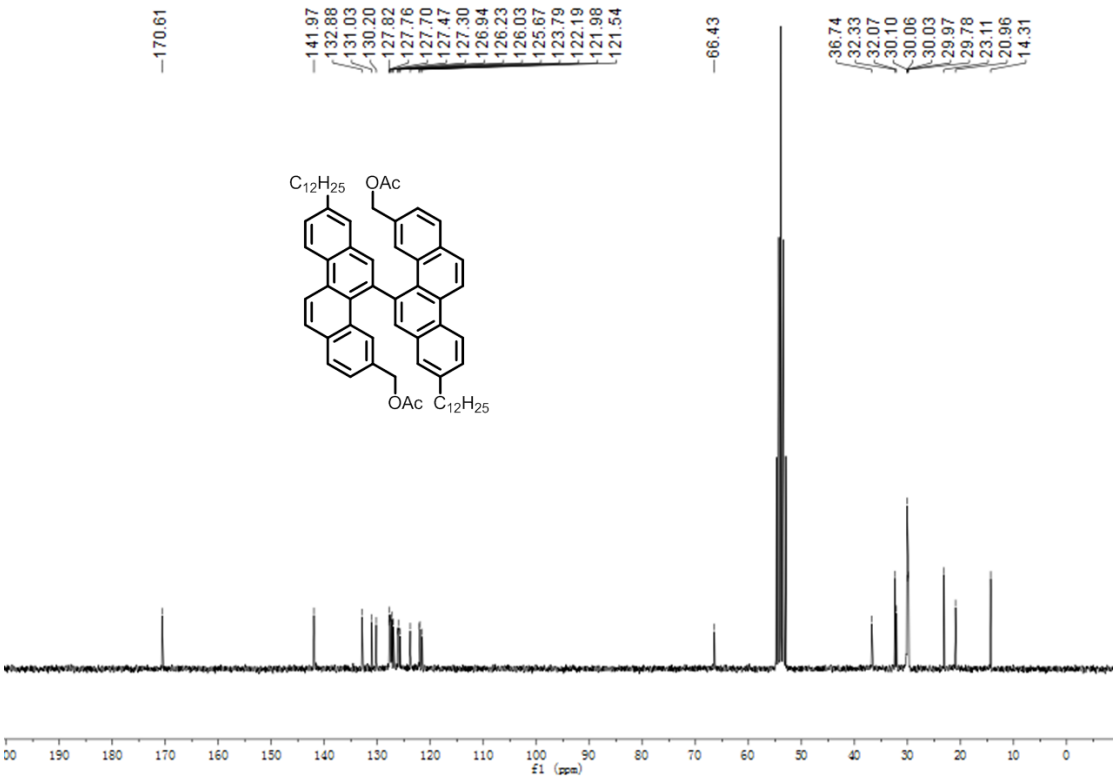

Figure S25. ^{13}C NMR spectrum of compound **7** in CD_2Cl_2 (62.5 MHz, 298 K).

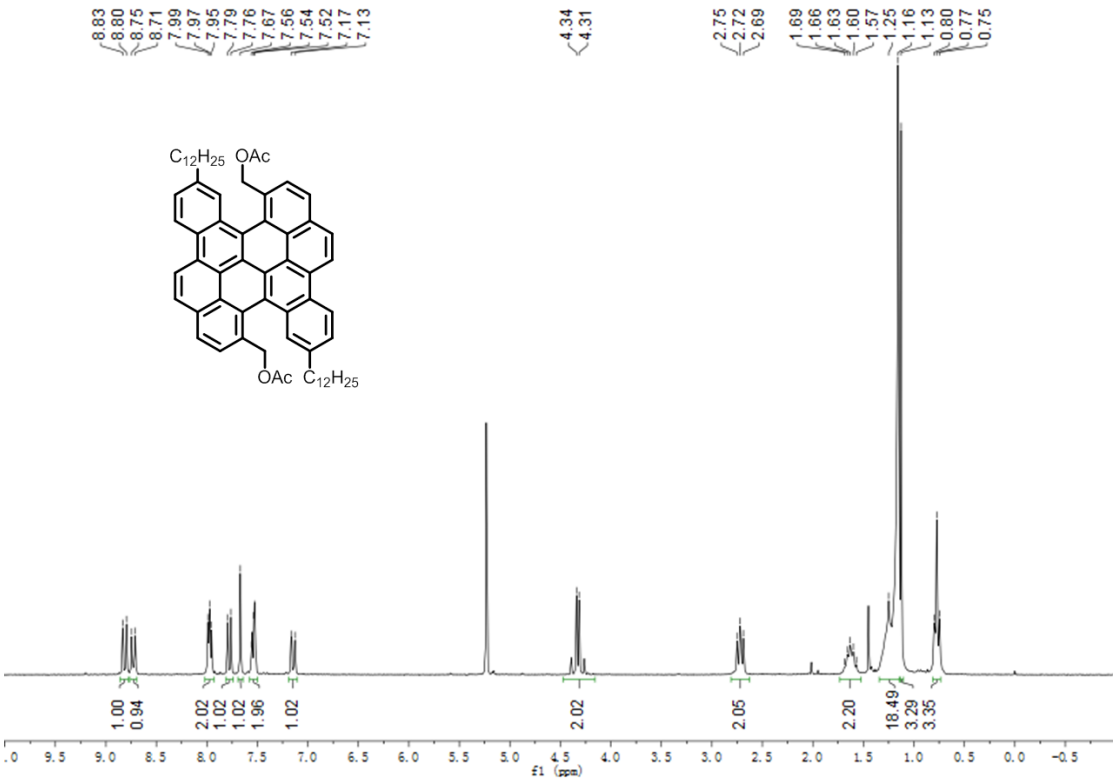

Figure S26. ^{1}H NMR spectrum of compound **8** in CD_2Cl_2 (250 MHz, 298 K).

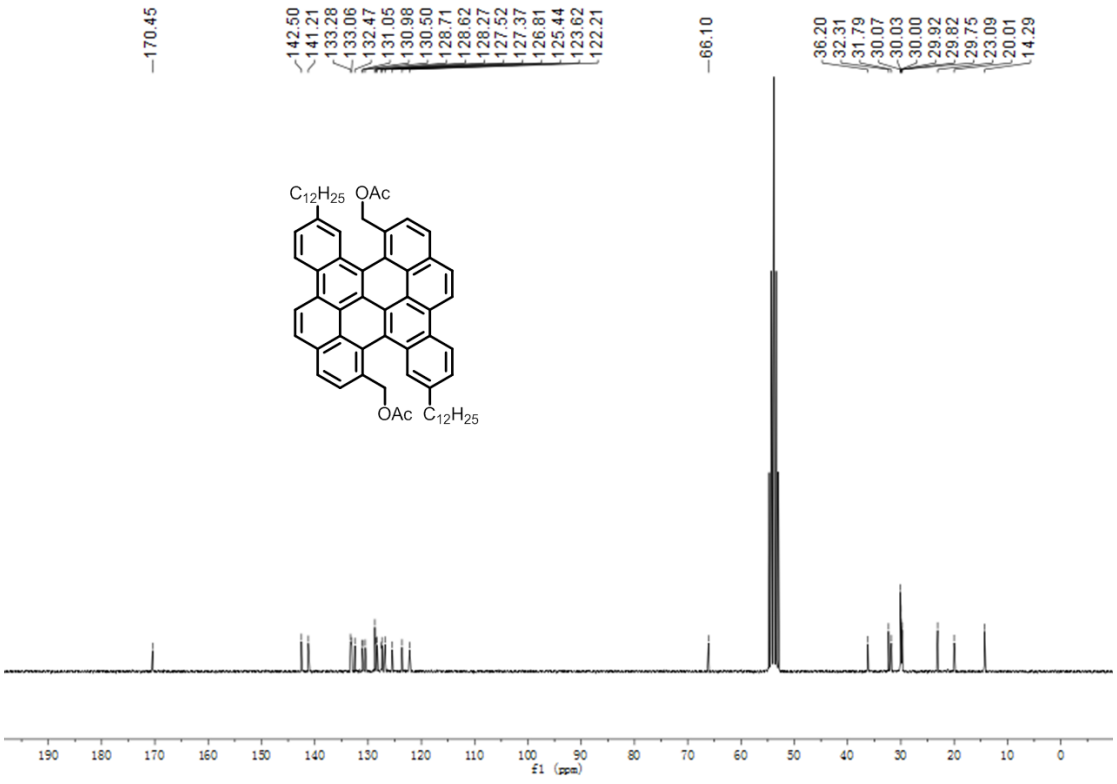

Figure S27. ^{13}C NMR spectrum of compound **8** in CD_2Cl_2 (62.5 MHz, 298 K).

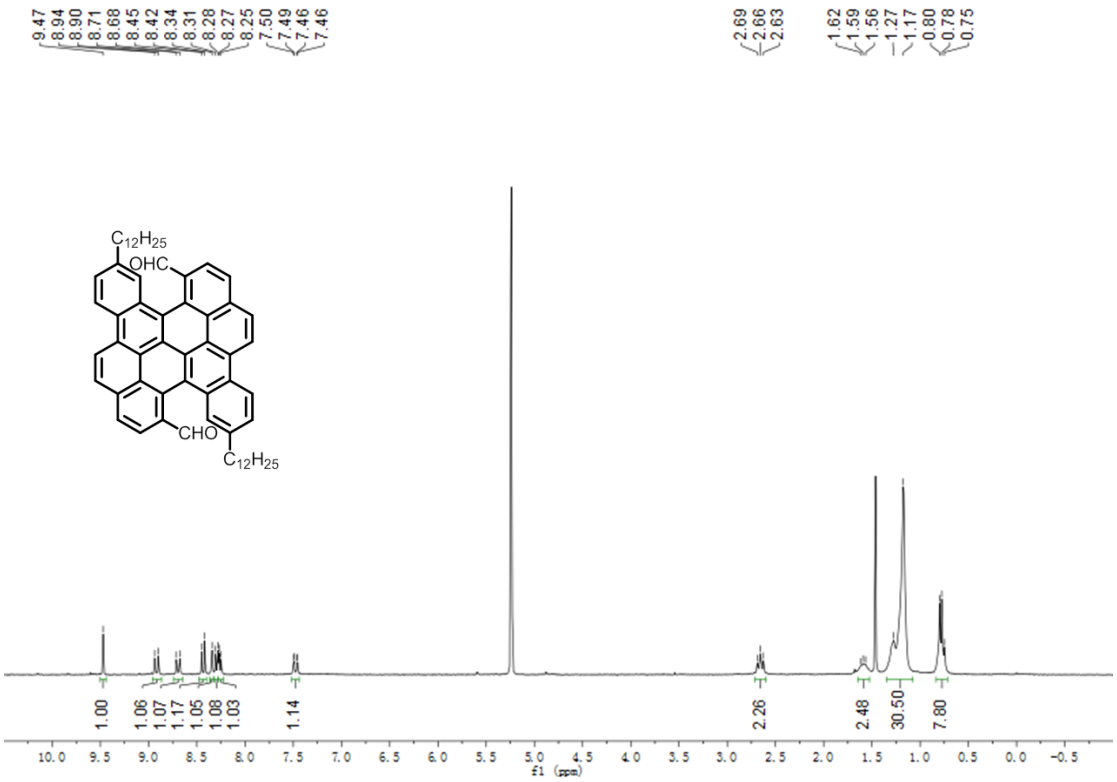

Figure S28. ^{1}H NMR spectrum of compound **9** in CD_2Cl_2 (250 MHz, 298 K).

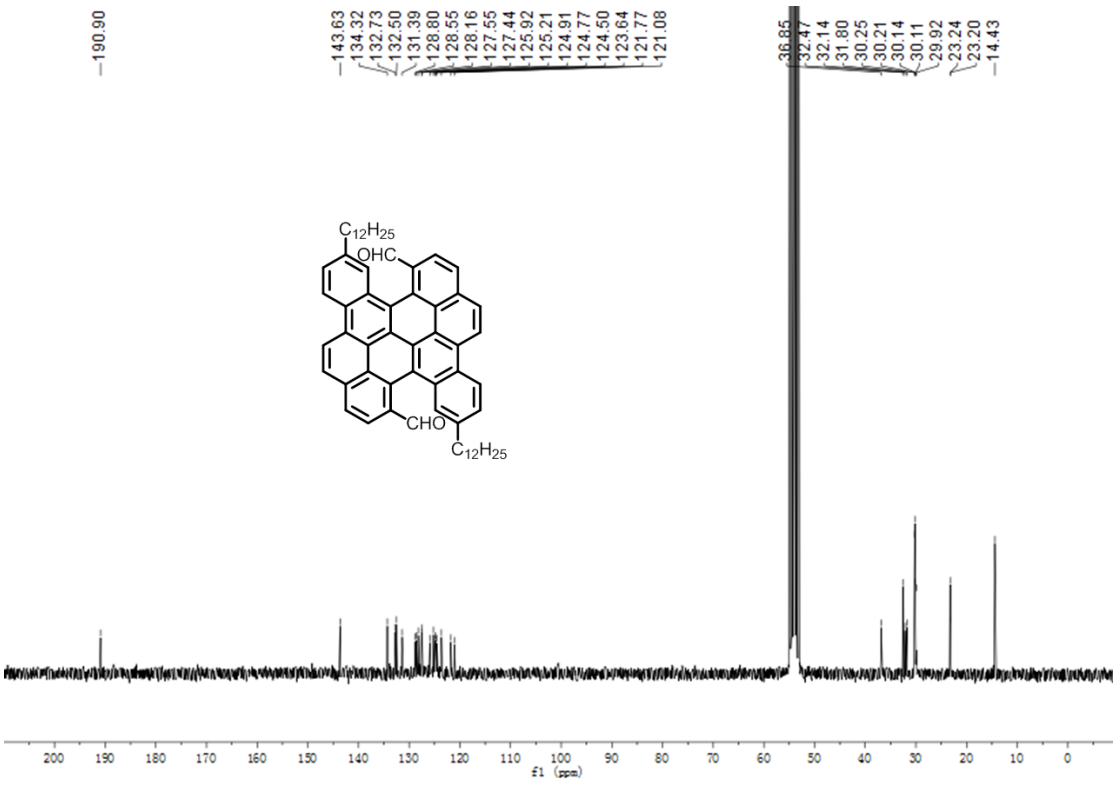

Figure S29. ^{13}C NMR spectrum of compound **9** in CD_2Cl_2 (62.5 MHz, 298 K).

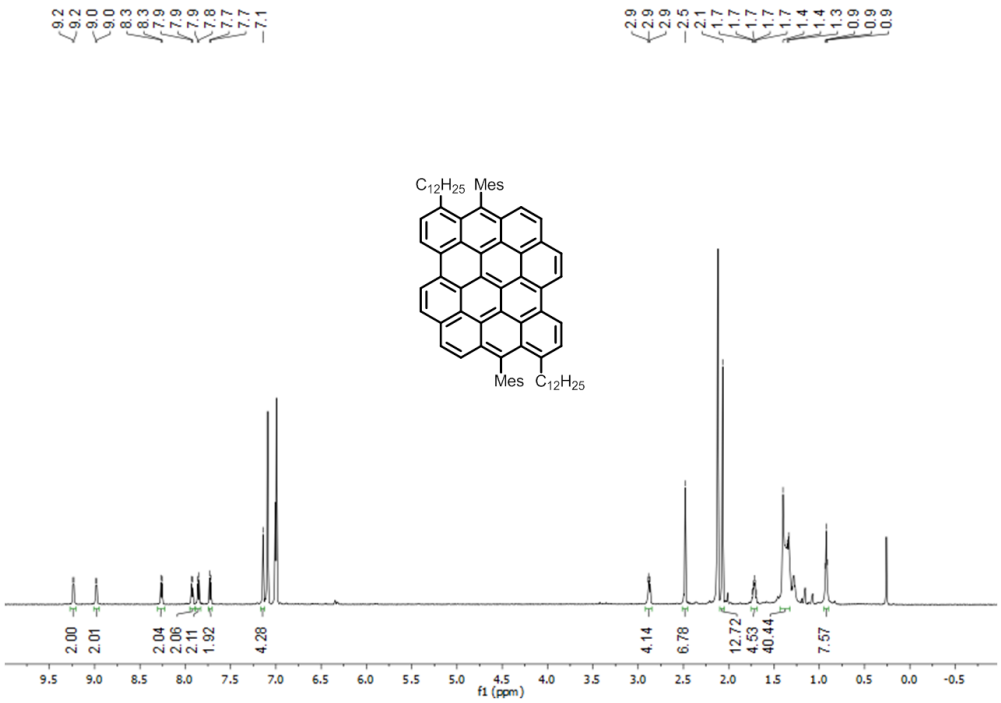

Figure S30. ^{1}H NMR spectrum of DBO **1** in toluene-d_8 (700 MHz, 373 K).

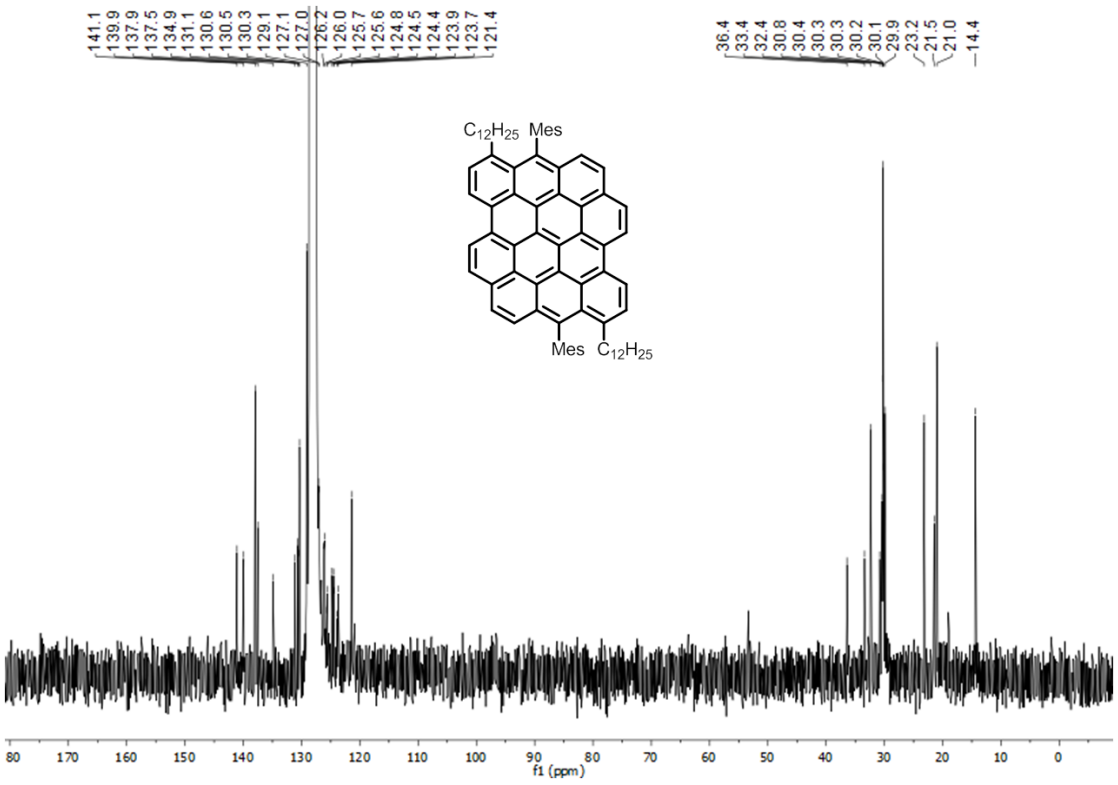

Figure S31. ^{13}C NMR spectrum of DBO **1** in benzene-d_6 (62.5 MHz, 298 K).

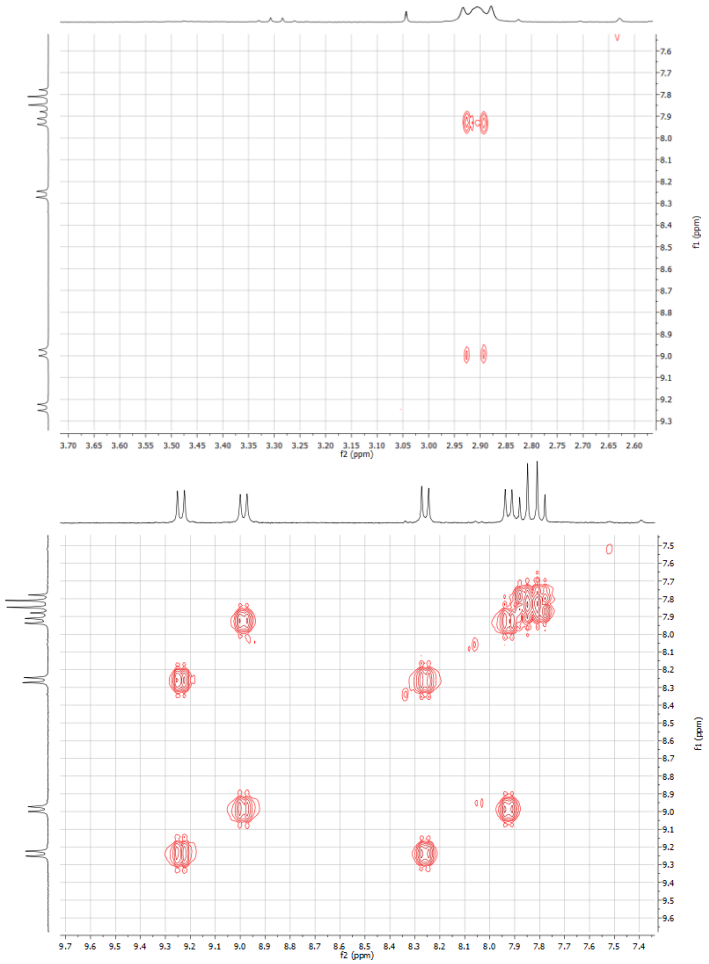

Figure S32. Aliphatic and aromatic area of the 1H,1H–COSY spectra of DBO 1 in toluene-d8 (300 MHz, 298 K).

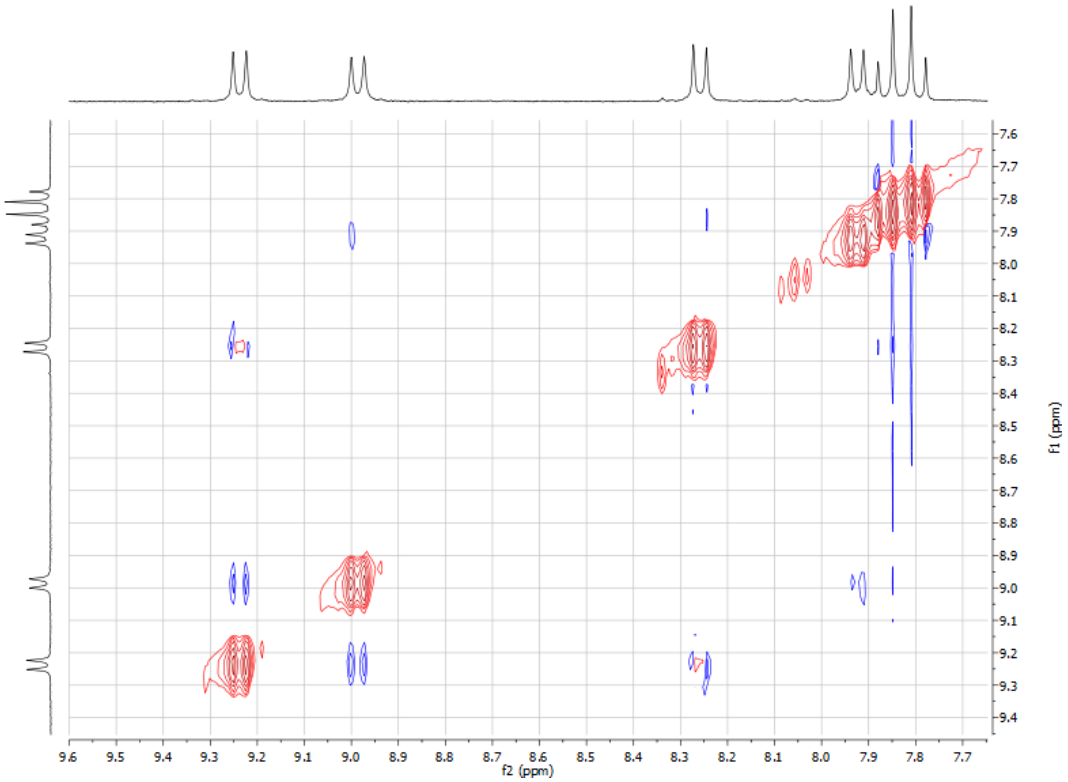

Figure S33. NOESY spectrum of DBO **1** in toluene-d_8 (300 MHz, 298K).

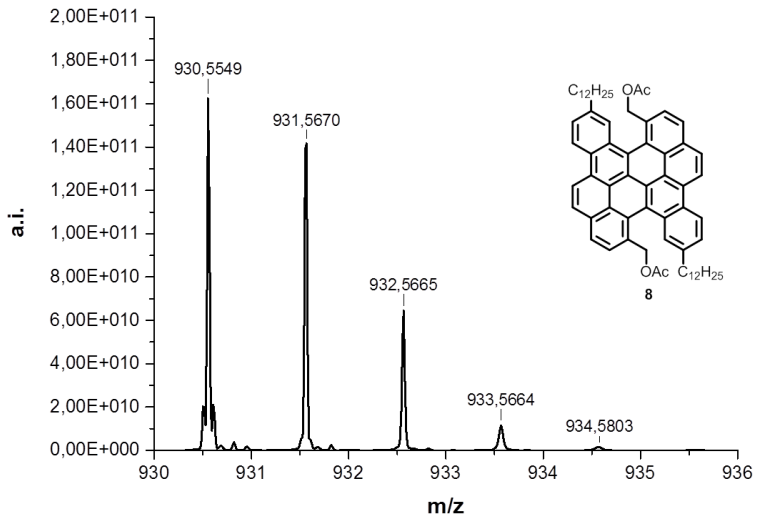

Figure S34. High-resolution MALDI-TOF mass spectrum of compound 8.

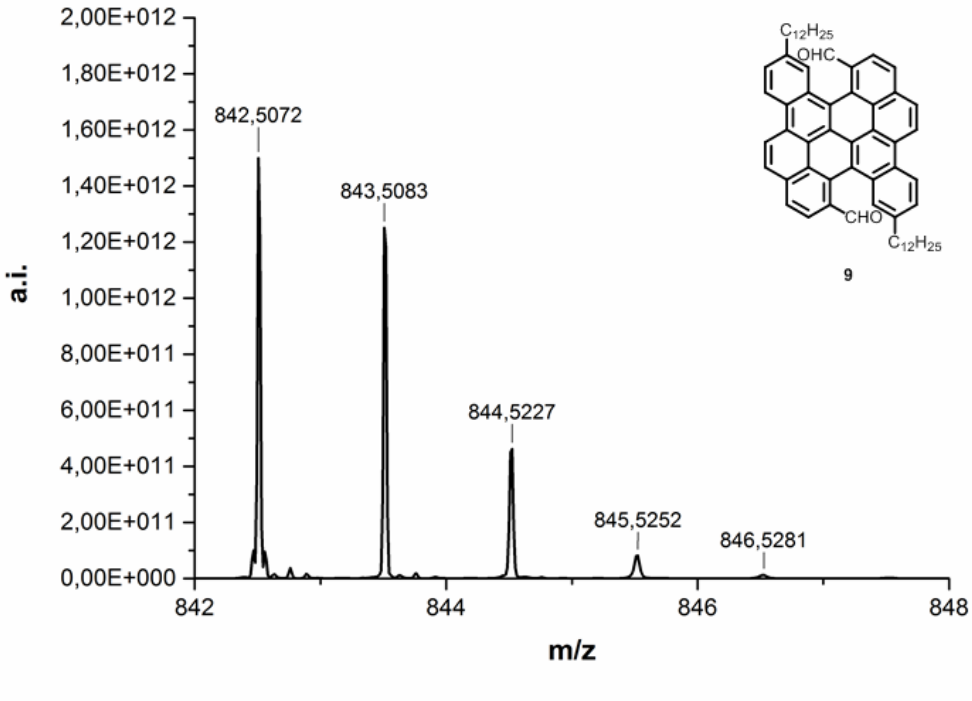

Figure S35. High-resolution MALDI-TOF mass spectrum of compound 9.

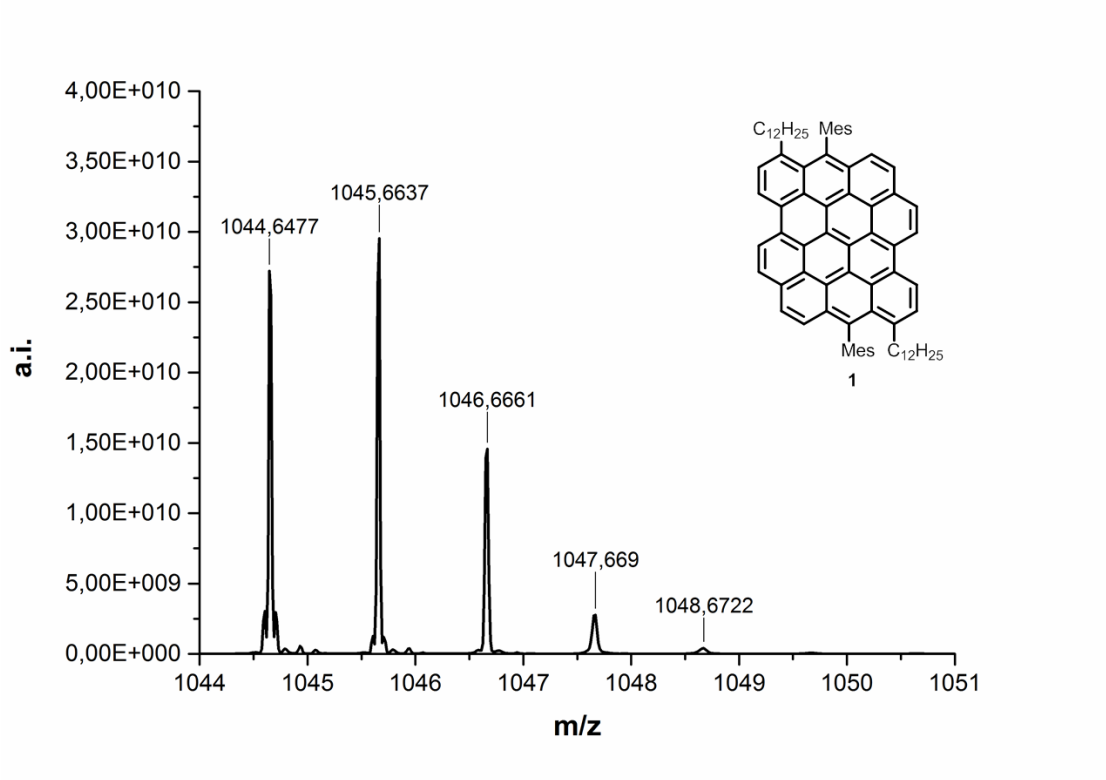

Figure S36. High-resolution MALDI-TOF mass spectrum of DBO 1.